AN ABSTRACT OF THE THESIS OF

Chia-Chang Hsu for the degree of Master of Science in Chemical Engineering

presented on December 1, 1993.

Title: Kinetic Study of $Si(NH)_2$ Synthesis via Low Temperature Vapor Phase Reaction of $SiCl_4$ and NH_3 in a Fluidized Bed Reactor

Redacted for Privacy

Abstract approved: _____

Shoichi Kimura

$Si(NH)_2$ synthesis via the vapor phase reaction of $SiCl_4$ and NH_3 was carried out at temperatures in the range of 280-353 K in a fluidized bed of inert Si_3N_4 particles. The reaction phenomena were observed through the glass wall of the fluidized bed reactor. It was found that fine Si_3N_4 powder with a mean particle size of 0.5 μm and a density of 2.9×10^3 kg/m^3 can collect product $Si(NH)_2$ more efficiently than large Si_3N_4 particles with a mean particle size of 370 μm and an apparent density of 2.63×10^3 kg/m^3. The effects of the concentration of $SiCl_4$, the mass of fluidized particles and the reaction temperature on the reaction rate were studied. A gas-phase reaction rate equation of pseudo-first order with respect to the $SiCl_4$ concentration was proposed. A plug flow reactor model with the proposed kinetics equation was developed to describe the reaction of $SiCl_4$ and NH_3 in the fluidized bed reactor. It was found that the reaction time needed to complete the reaction was on the order of seconds and almost a 100% of product $Si(NH)_2$ was collected by fluidizing Si_3N_4 fine powder. The apparent activation energy was evaluated to be 8.40 kJ/mol in the temperature range of 280-320 K.

Kinetic Study of $Si(NH)_2$ Synthesis via Low Temperature Vapor Phase Reaction of $SiCl_4$ and NH_3 in a Fluidized Bed Reactor

by

Chia-Chang Hsu

A THESIS

Submitted to

Oregon State University

in partial fulfillment of

the requirements for the

degree of

Master of Science

Completed December 1, 1993

Commencement June 1994

APPROVED:

Redacted for Privacy

Professor of Chemical Engineering in charge of major

Redacted for Privacy

Head of department of Chemical Engineering

Redacted for Privacy

Dean of Graduate School

Date thesis is presented December 1, 1993

Typed by researcher for Chia-Chang Hsu

TABLE OF CONTENTS

LIST OF FIGURES

NOMENCLATURES

A_b	cross-sectional area of the fluidized bed, m^2
C_{A0}	inlet concentration of $SiCl_4$ vapor, $kmol/m^3$
C_A	outlet concentration of $SiCl_4$ vapor, $kmol/m^3$
d_p	particle size, μm
E	apparent activation energy, kJ/mol
F	total volumetric flow rate of gases entering the reactor, m^3/s
f	collecting efficiency of product fine powder
$\Delta G^0_{R,298}$	Gibbs free energy, kJ/mol
g	acceleration of gravity, m/s^2
H	bed height, m
$\Delta H^0_{R,298}$	enthalpy, kJ/mol
k_A	apparent rate constant of the pseudo-first order reaction with respect to $SiCl_4$, /s
N_{Cl}	molar content of chlorine in a sample, mole
ΔP	pressure drop across the bed of solids, Pa
R_d	rate of $SiCl_4$ deposition, mol/kg s
r_A	rate of reaction, mol/s
t	reaction time, s
u_0	superficial velocity, m/s
u_{mf}	apparent minimum fluidizing velocity, m/s
V	volume of the bed, m^3
W_{b0}	initial mass of the bed, kg
W_b	average mass of the bed over the reaction period, kg
W_C	cumulative mass, kg
w	mass of the sample particles, kg
X_A	actual conversion of $SiCl_4$
X_A'	apparent conversion of $SiCl_4$

Greek letters

ε_A	overall void fraction of the bed
ρ_s	density of particles, kg/m^3
τ	resistance time of gaseous reactants, s

KINETIC STUDY OF $Si(NH)_2$ SYNTHESIS VIA LOW TEMPERATURE VAPOR PHASE REACTION OF $SiCl_4$ AND NH_3 IN A FLUIDIZED BED REACTOR

CHAPTER 1

INTRODUCTION

Thermal decomposition of silicon diimide ($Si(NH)_2$) is considered to be the most successful approach in the production of high purity α-form silicon nitride (α-Si_3N_4) [1], which is a high-temperature material for many engineering applications, *e.g.*, gas turbines and aerospace applications. $Si(NH)_2$, the precursor of Si_3N_4 synthesized via low temperature reaction of $SiCl_4$ with NH_3, plays an important role in this method [2].

Generally, $Si(NH)_2$ can be synthesized from $SiCl_4$ and NH_3 in gas phase, liquid phase, or gas-liquid interphase as

$$SiCl_4 + 6\,NH_3 \rightarrow Si(NH)_2 + 4\,NH_4Cl$$

Whenever liquid phase is involved, either in a liquid-liquid system or in a gas-liquid system, high purity $Si(NH)_2$ powder can be obtained by washing out the by-product, NH_4Cl, with liquid NH_3, and then high quality α-Si_3N_4 can be produced by calcining $Si(NH)_2$ at a temperature over 1273 K. The heat of vaporization of a liquid is utilized to control the reaction temperature, which is the major reason why a liquid is used in the system. However, these Si_3N_4 production processes are not economically attractive

due to the high operation cost associated with the NH_3 washing procedures. To reduce the production cost, gas phase reaction, in which solid products precipitate from the gaseous reactants and no solvent washing is required, has been considered as an alternative.

Nevertheless, the gas phase reaction also has major disadvantages. It has been reported that several problems are encountered in carrying out the gas phase reaction of $SiCl_4$ with NH_3. A high chlorine content in the primary $Si(NH)_2$ product may subsequently affect the quality of final product α-Si_3N_4 and that $SiCl_4$ and NH_3 vapors can react instantaneously at the outlets of reactant supply lines, thus forcing the reaction to be terminated in a short period of time because of the plugging problem.

Wang [3] found that the content of chlorine as an impurity in the final product, Si_3N_4, can be significantly reduced by controlling the reaction temperature and the following heat treatments for the precursor, $Si(NH)_2$. The plugging problem also can be solved by specially designing a feeding system [4]. These technologies to overcome the disadvantages of the gas phase reaction are employed in the present study.

From a view point of reaction engineering, a fluidized bed reactor is ideal for producing solids and for rapid gas phase reactions with large heat released, both of which are typical characteristics of the gas phase reaction of $SiCl_4$ and NH_3. Because both the products, $Si(NH)_2$ and NH_4Cl, are solids precipitating from the gaseous reactants, inert particles being fluidized may collect all the products. Thus, in a fluidized bed, the inert particles are allowed to expose their surface for solid-product collection and the heat of reaction can be simply removed by the fluidizing gas. The

products collected by the inert particles can be heated to remove NH_4Cl at 773 K and thermally decomposed into Si_3N_4 at 1273 K. If Si_3N_4 particles are used as inert, a fluidized bed reactor is able to prepare Si_3N_4 particles coated with $Si(NH)_2$ by carrying out this gas phase reaction. These composite particles can then be calcined into pure Si_3N_4 via the thermal decomposition in other fluidized beds operated at higher temperatures. With recycling some of these Si_3N_4 particles, a continuous fluidized-bed process can be developed to manufacture high quality Si_3N_4 powder.

The study presented in this thesis primarily focuses on the synthesis of $Si(NH)_2$ via the gas phase reaction of $SiCl_4$ and NH_3 in a fluidized bed reactor with Si_3N_4 particles as inert fluidizing media. The objectives of this research are:

1. To design a fluidized bed reactor which can be operated for a period of time long enough for collecting data,
2. To choose a right size of inert Si_3N_4 particles for collecting most of the products,
3. To inspect the fluidization phenomena,
4. To develop a model to describe the kinetics of $Si(NH)_2$ formation.

The results of this study will provide very useful information in developing an economical process for producing Si_3N_4.

There are five chapters in the thesis. Chapter 2 describes a literature review on the relevant work about the reaction chemistry, fluidization phenomena and the applications of fluidized beds to chemical vapor deposition (CVD) reactions where solid products precipitate from gaseous reactants. Also included are the comparison of different $Si(NH)_2$ synthesis-routes and calcine processes. Chapter 3 presents a detailed description of equipment design, experimental procedures and chemical analysis. The

experimental results are analyzed and discussed in Chapter 4. A kinetic model to describe the reaction of $SiCl_4$ with NH_3 in a fluidized bed is proposed and tested in this chapter. Finally, Chapter 5 summarizes the results of this work and recommendations for future work.

CHAPTER 2

LITERATURE REVIEW

2.1 Reaction Chemistry and Synthesis-Routes of $Si(NH)_2$

2.1.1 Reaction chemistry

The reaction of $SiCl_4$ with NH_3 at the room temperature was investigated for the first time by Billy *et al.* in 1959 [5]. They obtained fine-grained, roentgen-amorphous white powder which was the most typical compound of $Si(NH)_2$. The reaction was proposed to be represented by

$$SiCl_4\,(g) + 6\ NH_3\,(g) \rightarrow Si(NH)_2\,(s) + 4\ NH_4Cl\,(s) \qquad (2.1)$$

or

$$SiCl_4\,(g) + 18\ NH_3\,(g) \rightarrow 1/x\ [Si(NH)_2]_x\,(s) + 4\ NH_4Cl{\cdot}3NH_3 \qquad (2.2)$$

$$\Delta H^\circ_{R,298} = -675.1\ \text{kJ/mol} \qquad (2.3)$$

$$\Delta G^\circ_{R,298} = -384.1\ \text{kJ/mol} \qquad (2.4)$$

where the products in reaction (2.2) are polymeric silicon diimide and ammonia chloride triammoniate. The enthalpy ($\Delta H^\circ_{R,298}$) and Gibbs free energy ($\Delta G^\circ_{R,298}$) for this reaction were estimated by Crosbie [6]. In general, this reaction proceeds rapidly and completely with a large exothermic heat of reaction. It is suggested that ammonia should be supplied in excess of the stoichiometric ratio in either reaction (2.1) or (2.2) to achieve high conversion of $SiCl_4$ [4].

$Si(NH)_2$ obtained from the reaction described above can then be used to synthesize Si_3N_4. Synthesizing Si_3N_4 via the thermal decomposition of $Si(NH)_2$

involves several reactions. First, the products from reaction (2.1) or (2.2) are heated to a temperature above 673 K in a stream of NH_3 gas for more than 2 hours to eliminate NH_4Cl via sublimation. During the sublimation of NH_4Cl, the diimide intermediates, $[Si_3(NH)_3N_2]_n$, are formed [7]. These intermediate products are then calcined to form amorphous Si_3N_4 at 1273 K. Finally, the α-Si_3N_4 is obtained by crystallizing the amorphous Si_3N_4 at temperatures above 1473 K [8, 9]. A series of reactions summarizing the process of thermal decomposition of $Si(NH)_2$ are shown below:

$$6[Si(NH)_2]_n + NH_4Cl \xrightarrow{673\ K} 2[Si_3(NH)_3N_2]_n + NH_4Cl\uparrow \xrightarrow{923\ K}$$

$$3[Si_2(NH)N_2]_n \xrightarrow{1273\ K} Si_3N_4\ (amorphous) \xrightarrow{1473\ K} \alpha\text{-}Si_3N_4 \qquad (2.5)$$

This research mainly focuses on the kinetics of $Si(NH)_2$ synthesis, as described by reaction (2.1) or (2.2). The thermal decomposition of $Si(NH)_2$ to form Si_3N_4, as described by reaction (2.5) is not included in this work.

2.1.2 Routes of synthesis

$Si(NH)_2$ has been prepared by researchers via three different routes: liquid-liquid, gas-liquid and gas-gas reactions.

Liquid-liquid reaction:

The problems often encountered in the $Si(NH)_2$ synthesis are the difficulty in removing heat generated by the extremely rapid exothermic reaction, the tendency that

product $Si(NH)_2$ plugs $SiCl_4$ supply lines, and the difficulty in separating $Si(NH)_2$ from by-product NH_4Cl. Yamada *et al.*[1, 2] developed a liquid-liquid interfacial reaction method to solve these problems. In this method, NH_3 reacts with $SiCl_4$ at the interface between a liquid NH_3 layer and an organic solvent layer which dissolves $SiCl_4$. The products precipitate as a solid mixture at the interface of these immiscible liquids. The reaction temperature may be controlled by the evaporation of NH_3. The mixture of reaction products needs to be washed out with an excess amount of liquid NH_3 to remove by-product NH_4Cl. After the washing, $Si(NH)_2$ is processed through heat treatments to form highly pure α-Si_3N_4 which has been regarded as Si_3N_4 of highest quality. However, this $Si(NH)_2$ synthesis route is not very economic because many operating steps are involved and organic solvent as well as a large quantity of liquid NH_3 are required.

Gas-liquid reaction:

The synthesis-route through gas-liquid reactions was first investigated by Billy [5] in 1959 and tested by Ford Motor Company in 1988 [10, 11]. $SiCl_4$ vapor generated by bubbling nitrogen carrier gas through liquid $SiCl_4$ is directed into a liquid NH_3 vessel for reaction. Heat generated by the reaction is removed by the evaporation of NH_3 under operating conditions at 5 atm and 273 K. Again, NH_4Cl must be removed from product $Si(NH)_2$ using 240 K liquid NH_3. Although α-Si_3N_4 is finally obtained by calcining $Si(NH)_2$, it has been reported that the quality of Si_3N_4 is lower than that produced by the liquid-liquid reaction.

Instead of using liquid NH_3 and vapor $SiCl_4$, Mazdiyasni *et al.* [9] and Mitomo *et al.* [12] used vapor NH_3 and liquid $SiCl_4$ to synthesize $Si(NH)_2$. The reaction is carried out by bubbling NH_3 gas through liquid *n*-hexane which contains dissolved $SiCl_4$ at 273 K. A white powder-mixture of $Si(NH)_2$ and NH_4Cl precipitates in *n*-hexane and then is isolated from the hexane solvent by distillation under a reduced pressure at 300 K. Following the sequence represented by equation (2.5), the isolated $Si(NH)_2$ is then calcined and crystallized into α-Si_3N_4 at temperatures higher than 1473 K.

Gas-phase reaction:

To avoid the operation for liquid-solid separation and to simplify the process, gas-phase routes for the synthesis of silicon diimide have been considered. Kasai *et al.* [8] prepared α-Si_3N_4 via the thermal decomposition of $Si(NH)_2$ synthesized by the gas-phase reaction.

Vapor $SiCl_4$, generated by bubbling N_2 through liquid $SiCl_4$, and NH_3 gas are introduced into a tubular reactor, through separate feed lines, operated at the room temperature. Upon the interaction of these vapors, a white powder-mixture containing $Si(NH)_2$ and NH_4Cl is produced via a CVD mechanism. NH_4Cl may be removed by heating the powder mixture at 673 K for 2 hours. The isolated $Si(NH)_2$ is then calcined to form highly pure α-Si_3N_4 in the presence of NH_3 at 1823 K for 1 hour.

Wang [3] has claimed that the content of chlorine in the final product Si_3N_4 prepared by this method can be reduced to a level below 100 ppm by carrying out the gas-phase reaction at a temperature in the range of 298-473 K. He also found that

impurity chlorine can not be reduced appreciably regardless of the following heat treatments when the reaction temperature is higher than 473 K. The present research aims to make full use of the advantage of the gas-phase reaction route carried out at low temperatures.

2.2 Reaction Kinetics and Mechanism of the Deposition Process

2.2.1 Reaction kinetics

Studies on the kinetics of the reaction of $SiCl_4$ with NH_3 have focused on the deposition of Si_3N_4 thin films on silicon substrates at high temperatures (973-1473 K), instead of the kinetics for $Si(NH)_2$ synthesis at low temperatures. Grieco *et al.* [13] determined the rate of Si_3N_4 film deposition by measuring the increase in film thickness during the reaction. From a log-log plot of the deposition rate against the partial pressure of $SiCl_4$, they found a kinetics of 0.8th order with respect to the partial pressure of $SiCl_4$. The activation energy of the reaction at high temperatures in the range of 973-1473 K was determined to be 62.7 ± 6.3 kJ/mol. Nevertheless, the kinetic study on the reaction of $SiCl_4$ with NH_3 to produce $Si(NH)_2$ at low temperatures around the room temperature has not been reported in literature yet. This thesis presents the results of the kinetic study on the $Si(NH)_2$ synthesis.

2.2.2 Mechanism of the deposition process

There are two different of mechanisms proposed for the deposition of Si_3N_4 via the reaction of $SiCl_4$ with NH_3 at high temperatures [14]. One is the heterogeneous reaction of the Langmuir-Hinscheloow type. The reaction has been believed to occur in an adsorbed layer on substrates, and the rate is usually determined by the degrees of coverage of the surface of a growing film with adsorbed $SiCl_4$ and NH_3 molecules. This mechanism is valid for the reactions under low pressures. The deposition of a Si_3N_4 thin film on Si substrates is a typical example. Another is the homogeneous reaction in gas phase, precipitating solid products. The reactants interact with each other in gas phase and then the dust-like products fall down to stick on the reactor surface. This mechanism is suggested to proceed under the conditions around the atmospheric pressure with high reactant concentrations. The production of Si_3N_4 powder via CVD reactions is a representative example.

Wang [3] conducted the CVD reaction of $SiCl_4$ with NH_3 in a 0.915 m long tubular reactor at one atmosphere. At 300 K, he found that the majority of product (75%) was carried out of the reactor by the gas flow and collected by a trap connected to the reactor, and the rest of the product (25%) deposited on the reactor wall down stream. It is suggested that light, fluffy, white powder, obtained both in the reactor tube and the trap, was produced via the homogeneous gas-phase reaction followed by the solid precipitation.

2.3 The Characteristics of Fluidizing Fine Particles

2.3.1 Particle classification

Geldart *et al.* [15] determined the characteristics of gas-solid fluidization on the basis of the size and density of particles. Geldart D particles, which have a large size and a high density, are spoutable and difficult to be fluidized. Usually, either large exploding bubbles form or severe channeling occurs in a fluidized bed of these particles. Particles with a size (d_p) between 40 and 500 μm and a density (ρ_s) between 1.4×10^3 and 4.0×10^3 kg/m^3 are classified as Geldart B, which can be fluidized smoothly. Bubbles are generated and rise faster than the interstitial gas velocities in a fluidized bed of these particles [16]. Geldart A particles, which have a size less than 40 μm and a density less than 1.4×10^3 kg/m^3, are easily fluidized at low gas velocities. Bubbling and entrainment sometimes occur in fluidizing these particles. Geldart C particles, which have a size less than 30 μm, are extremely difficult to fluidize, because the inter-particle forces are too strong to be overcome by the hydrodynamic forces exerting on the particles. When an ordinary fluidization technique is applied, the whole bed rises as a plug in a small bed in diameter. The rising velocity of bubbles cannot be determined easily, and the entrainment of fines is also significant once these Geldart C particles are fluidized.

2.3.2 Fluidizing Si_3N_4 powder

Some studies have demonstrated that fine particles, classified as Geldart C, can be fluidized if the particles grow in size by self-agglomeration [17, 18]. It has been reported that ultrafine Si_3N_4 powder (d_p= 0.13-0.50 μm, $\rho_s = 2.91\times10^3$ kg/m^3) can be fluidized [19, 20]. Self-agglomeration takes place when the van der Waals force among adjacent particles and the shearing force, generated by bubble movement, are in dynamic equilibrium. Once sub-micron fines aggregate to form big clusters, it becomes possible to fluidize the fines which behave like group A particles.

Even fines are fluidized in the form of big agglomerates, the entrainment of fines is also significant in the fluidization. Liu & Kimura [20] have reported that, in the fluidization of a mixture of large particles and fines, entrained fines come mainly from two parts: (1) elutriable freely moving fines, which may be continuously and steadily generated from agglomerates of fines, and (2) fines attached to the large particles, being generated due to attrition. In the current case, the elutriable fines may also include product fines produced by the reaction between $SiCl_4$ and NH_3.

2.4 CVD Reactions in Fluidized Beds

The fluidization has been applied to many CVD systems, such as the growth of seed particles, modification of powder surface, introduction of specific function to solids, and formation of fine particles by coagulation [21]. Two successful examples of fluidizing Si_3N_4 fine powder are described below.

In the application to modifying powder surface, Morooka *et al.* [4] developed a CVD process to produce composite particles in a fluidized bed. TiN particles, generated by the ammonolysis reaction of $TiCl_4$, were deposited on the surface of fluidized Si_3N_4 fines. The composite particles with an average size of 50 μm were obtained in the form of agglomerates.

The production of Si_3N_4 powder by the reaction of $SiCl_4$ with NH_3 in a fluidized bed was first developed by Marosi [22]. They fluidized amorphous Si_3N_4 powder smaller than 4 μm in diameter as seed particles for the reaction. In order to eliminate NH_4Cl from the fluidized bed, the reaction was conducted at temperatures over 773 K. With a cyclone for collecting entrained fine particles, this bed could be continuously operated for 21 hours. Final product having an average particle size of approximately 20 μm and containing 58.8% Si and 39% N was obtained.

The study described in this thesis focuses mainly on the kinetics of the gas phase reaction of $SiCl_4$ with NH_3 at temperatures around the room temperature in a fluidized bed reactor. A fluidized bed reaction system was designed and constructed for this study. Two kinds of Si_3N_4 particles, one in Geldart B ($\rho_s = 2.63\times10^3$ kg/m^3, d_p = 370 μm) and the other in Geldart C ($\rho_s = 2.90\times10^3$ kg/m^3, d_p = 0.50 μm), were fluidized to investigate the capability of collecting solid products. NH_3 was supplied in excess of the stoichiometric ratio to convert most of $SiCl_4$ [3, 22]. The objective of this study is also to develop a kinetic model for the reaction between NH_3 and $SiCl_4$ vapors at low temperatures (280-353 K). The literature review described above provided sufficient background information for conducting the study.

CHAPTER 3

EXPERIMENTAL EQUIPMENT AND PROCEDURES

Figure 3.1 shows the schematic diagram of the reaction system used in this study. The system consists of an NH_3 gas supply, a $SiCl_4$ vapor supply, a fluidized bed reactor for the NH_3-$SiCl_4$ reaction, and a sampler to collect product $Si(NH)_2$ powder.

Si_3N_4 particles which served as inert particles for the collection of product $Si(NH)_2$ were charged into the reactor. Through the distributor at the bottom of the reactor, NH_3 gas diluted with oxygen-free N_2 was fed to fluidize the inert particles. $SiCl_4$ vapor, generated by bubbling oxygen-free N_2 through a reservoir of liquid $SiCl_4$, was fed through concentric tubes into the fluidized bed for reaction. The separate feeding lines for the reactants were designed to prevent solid products from plugging the NH_3 gas distributor. The reaction temperature in the fluidized bed was controlled by a furnace with a temperature controller or by an ice bath, depending upon the temperature to be set. The outlet of the fluidized bed reactor was divided into two streams: one connected to a flask with a filter to trap very fine particles being blown out of the reactor by the nitrogen carrier gas, and the other connected to a flask to periodically sample products from the reactor for analysis. By opening the sampling valve, closing the vent valve, and inserting the sampling tube to the top of the dense zone of fluidized bed, product powder could be sampled together with inert particles easily when needed. The details of this reaction system, as well as chemicals and experimental procedures used in this study, are described in the following sections.

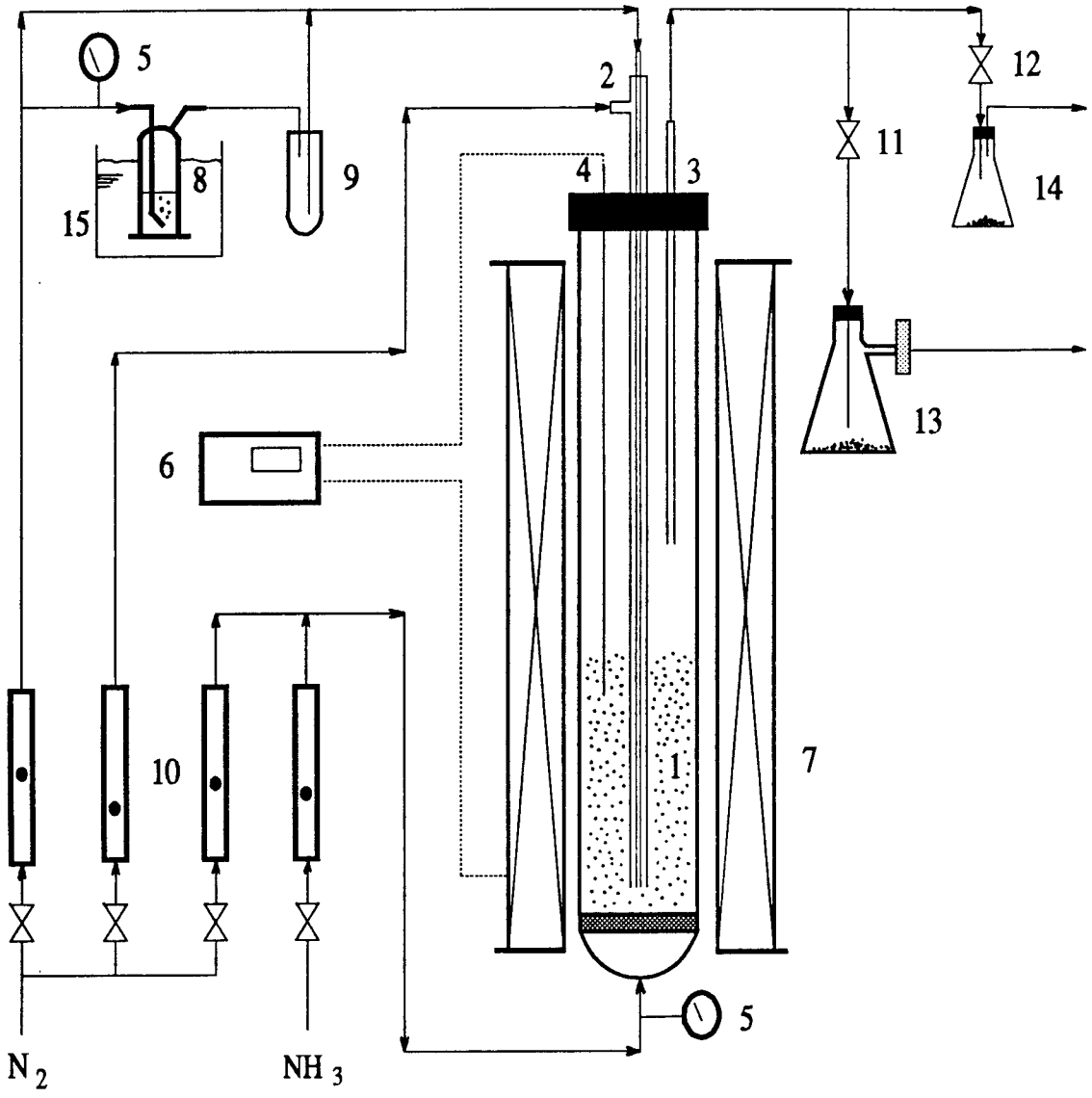

1. Fluidized bed reactor
2. $SiCl_4$ supply pipe
3. Sampling tube
4. Thermocouple
5. Pressure gauges
6. Temperature controller
7. Furnace/ ice bath
8. $SiCl_4$ reservoir/ bubbler
9. Trap
10. Flowmeter
11. Vent valve
12. Sampling valve
13. Trap flask
14. Sampling flask
15. Ice-water bath

Figure 3.1 Schematic diagram of equipment.

3.1 Reaction System Set-up

3.1.1 Fluidized bed reactor

The fluidized bed reactor consists of two major parts, (1) a reactor column with an NH_3/N_2 gas distributor and an NH_3/N_2 gas intake adaptor, and (2) a stopper assembly to seal the upper end of the reactor column and also to permit the $SiCl_4/N_2$ gas entrance, the thermocouple insertion, the N_2 carrier gas release, and the product sample collection. The reactor column is made of a glass tube of 4.2 cm i.d. and 55 cm long. The NH_3 gas distributor, welded onto the lower portion of the reactor column, is a 2.5 mm-thick sintered glass disc with pores of an average size of 2.0 μm. The NH_3/N_2 gas intake adaptor is a glass ball-socket joint welded at the bottom of the reactor column to be connected to the NH_3/N_2 source line. The fluidized bed reactor is corrosion-resistant against the reactants and allows measurements of bed height by direct observation through the glass wall.

The upper stopper is made of Teflon. Through the stopper, a $SiCl_4/N_2$ supply pipe, made of two concentric stainless steel tubes, is connected to the $SiCl_4$ vapor supplying source. N_2 and $SiCl_4/N_2$ mixture gas are fed into the reactor through the annulus and the inner tube of the concentric tube-assembly, respectively. The outlets of the concentric tubes are placed 1.0 cm above the NH_3 gas distributor. This concentric tube-assembly was designed to prevent solid products from depositing at the outlet of the $SiCl_4/N_2$ feeding line.

A k-type thermocouple to measure the reaction temperature and a stainless steel tube to sample product powder are also inserted through the upper stopper. The

thermocouple probe is located 10 cm above the NH_3 gas distributor. The sampling tube made of a 0.64 cm i.d. stainless steel tube is held using a Swagelok stainless steel male connector with an O-ring seal. The hole of the male connector is designed to allow the sampling tube to slide up and down within the column during sampling operations.

3.1.2 $SiCl_4$ reservoir with trap

$SiCl_4$ vapor to be supplied to the fluidized bed reactor was generated by bubbling nitrogen gas at a constant flow rate through a liquid $SiCl_4$ in a reservoir. The $SiCl_4$ reservoir is made of glass with a sintered glass sparger for nitrogen bubbling. An ice/water bath maintains the temperature of liquid $SiCl_4$ at 273 K. Because the saturated vapor pressure of $SiCl_4$ at 273 K is known to be 10.3 kPa, assuming that the nitrogen gas is saturated with $SiCl_4$ vapor allows one to determine the molar flow rate of $SiCl_4$ fed into the fluidized bed. A trap installed in the stream between the bubbler and the $SiCl_4$ supply pipe prevents product powder from returning into the bubbler.

3.1.3 Controller, furnace and ice bath

A PID controller (model number CN 9000A, purchased from Omega Engineering, Inc.) connected with a thermocouple was used to display the reaction temperature and to adjust the power to be supplied to the furnace (model number M-2724, Hevi-duty Electric Co., Milwaukee, Wisconsin) with heating elements made of a

nickel and chromium alloy. The maximum achievable temperature of the furnace is 1273 K and the maximum available electrical power is 2 kW.

A column, made of a PVC tube of 10 cm i.d. and 50 cm long with a closed bottom, was used as an ice/water bath to keep the fluidized bed reactor at 280 K. The NH_3/N_2 intake adaptor was connected with the NH_3/N_2 gas supply source through a hole drilled on the bottom of the ice/water bath, which was sealed with a rubber stopper.

3.1.4 Sampling flask and trap flasks

A Pyrex 500 ml filtering flask was connected to the sampling tube for sampling product powder from the top of the fluidized bed. A couple of Pyrex 1000 ml filtering flasks with tubulation were used alternatively for collecting carryover fines. The side arm of each flask was connected to a filter in order to trap all the powder. The product powder collected in the sampling flask and the carryover fines collected by the trap flasks with filters were weighed and then chemically analyzed.

3.2 Chemicals

There were two kinds of Si_3N_4 powder employed as inert particles in the reaction. Si_3N_4 fine powder with a mean particle size (d_p) of 0.5 μm and a density (ρ_s) of 2.90×10^3 kg/m^3, classified as Geldart C particles, and large particles with d_p = 330 μm and $\rho_s = 2.63\times10^3$ kg/m^3, classified as Geldart B particles, were both offered by Shin Etsu Chemical Company, Ltd. Liquid $SiCl_4$ (99%) used as one of the reactants,

solid $AgNO_3$ (99%) and K_2CrO_4 (98%) used for chemical analysis were all of analytical grade, purchased from Aldrich Chemical Company, Inc. N_2 gas (standard-grade) and NH_3 gas (99.9%) were supplied from a local dealer. Distilled water was provided by the Department of Chemistry, Oregon State University.

3.3 Experimental Procedures

3.3.1 Preliminary experiments

In order to make sure that particles are well-fluidized in the reactor, measuring the apparent minimum fluidizing velocities (u_{mf}) is always required even when some suggested values are available in literature [19, 20]. Generally, u_{mf} can be determined by plotting the pressure drop (ΔP) across the bed of solids versus superficial gas velocity (u_0) [24]. The pressure gauge installed on the NH_3/N_2 source line, as shown in Figure 3.1, was used to measure the total pressure drop through the NH_3 gas distributor and across the bed. ΔP was then evaluated as the difference between the total pressure drop across the fluidized bed with solids and it across the empty bed. Total pressure drops were measured at velocities u_0 as they were increased (aeration) from zero to 0.34 m/s and then at velocities u_0 as they were decreased (deaeration) back to zero. The total pressures were recorded after the fluidization was maintained at each gas velocity for 5 minutes. Both Si_3N_4 fine powder and large particles described in the previous section were investigated.

3.3.2 Experimental procedures

A pre-weighed amount of inert Si_3N_4 particles were first fluidized by nitrogen at a velocity of 1.5 times u_{mf}. Meanwhile, N_2 gas to bubble through liquid $SiCl_4$, at a volumetric flow rate of 8.3×10^{-7} m^3/sec, by-passed the $SiCl_4$ reservoir and flowed into the bed through the inner tube of the $SiCl_4$ supply pipe. N_2 gas at a constant flow rate of 3.3×10^{-6} m^3/s was also directed through the annulus of the $SiCl_4$ supply pipe into the reactor. At the beginning of each run, the inert particles were fluidized with no reactants supplied for 45 minutes. This preparation step assured the inert powder, in particular, to be agglomerated to a fluidizable size and the fluidized bed to be stabilized. To start the reaction, NH_3 gas, at a flow rate of 2.5×10^{-6} m^3/s, was added to the fluidizing N_2 gas. At the same time, the N_2 gas by-passing liquid $SiCl_4$ was switched to pass through the $SiCl_4$ reservoir to carry $SiCl_4$ vapor into the reactor. The total gas flow rate was set at 1.05×10^{-4} m^3/s for the fine Si_3N_4 powder and 3.08×10^{-4} m^3/s for the large Si_3N_4 particles. A sample of approximate one gram of solids was taken from the bed every 20 minutes for chemical analysis. The trap flasks for collecting carryover were replaced alternatively every 15 minutes. The increase in the total mass of each trap flask was measured to determine the entrainment from the fluidized bed. The reaction was carried out for 100 minutes.

The preliminary experiments for testing the influence of the size of inert particles on the efficiency of collecting solid products were conducted using the fine and large inert Si_3N_4 particles. Based on the experimental results, the fine inert Si_3N_4 powder which gave a higher efficiency was chosen to study the reaction kinetics.

The concentration of $SiCl_4$ was varied from 9.60×10^{-6} kmol/m^3 to 4.99×10^{-5} kmol/m^3 to see the influence of the $SiCl_4$ concentration on the rate of $Si(NH)_2$ deposition onto the inert particles. The initial bed mass of the inert particles was changed in the range of 0.080-0.180 kg to test the reaction kinetics of $Si(NH)_2$ synthesis in a fluidized bed reactor. The reaction temperature was set in the range of 280-353 K in order to investigate the temperature dependence of the reaction rate.

3.3.3 Chemical analysis

According to reaction (2.1) or (2.2), chloride ion is the only chemical component in product mixtures which can be quantified easily and precisely by a simple chemical analysis. The amount of desired product, $Si(NH)_2$, can be evaluated by dividing the amount of chloride ion by 4, assuming that one mole of $Si(NH)_2$ is always associated with four moles of NH_4Cl according to the stoichiometry.

The chlorine contents of samples were determined by the Mohr's titration method [23]. The method uses a $AgNO_3$ solution as a titrator and K_2CrO_4 as an indicator. There are two kinds of precipitates formed during the titration.

$$Cl^- + Ag^+ \rightarrow AgCl \qquad \text{(a white precipitate)} \qquad (3.1)$$

$$CrO_4^{-2} + 2Ag^+ \rightarrow Ag_2CrO_4 \qquad \text{(a yellow-orange precipitate)} \qquad (3.2)$$

Since AgCl is less soluble than Ag_2CrO_4, the latter can not show up until chloride ions have been consumed completely by silver ions. Therefore, the end point is marked by the first formation of the yellow-orange precipitate of Ag_2CrO_4.

After measuring sample mass, each sample was dissolved in Cl^--free distilled water for 5 hours. A few drops of the indicator were added to the solution. The

solution with chloride ions was then titrated by an aqueous 0.01 N $AgNO_3$ solution until sharp the yellow precipitate was observed under yellow light. A blank test on the indicator was also carried out when the 0.01 N silver nitrate solution was used.

CHAPTER 4

RESULTS AND DISCUSSION

4.1 The Measurement of Minimum Fluidizing Velocities

Figures 4.1 and 4.2 show the diagrams of the pressure drop across the fluidized bed varying with the velocity of fluidizing gas for large and fine Si_3N_4 particles, respectively. Here, the pressure drop is normalized by dividing the measured data by the gravitational force exerting on the bed-solids per unit cross-sectional area, $\Delta P/(W_{b0}\, g/A_b)$. These diagrams can be used to determine the minimum fluidizing velocities (u_{mf}) for particles [20, 24]. Figure 4.1 shows that the normalized pressure drops for deaeration are around unity while particles are being fluidized and then slip back to the origin when the fluidizing velocity is decreased. Also, the normalized pressure drops in aeration and deaeration do not deviate from unity in the fluidizing region. This result indicates that there is no entrainment in the large Geldart B Si_3N_4 particles. The minimum fluidizing velocity u_{mf} for the large can easily be determined to be 0.135 m/s.

Unlike the pressure drop data shown in Figure 4.1, the pressure drop in deaeration in Figure 4.2 shows a small negative deviation from unity in the fluidizing region. The decreased pressure drop is attributed to the particle entrainment after a bed was fluidized for a certain period of time. Here, the pressure drop data in the deaeration operation were used as the bases to determine the minimum fluidizing velocity. Although there was still uncertainty, u_{mf} = 0.045 m/s was employed in this

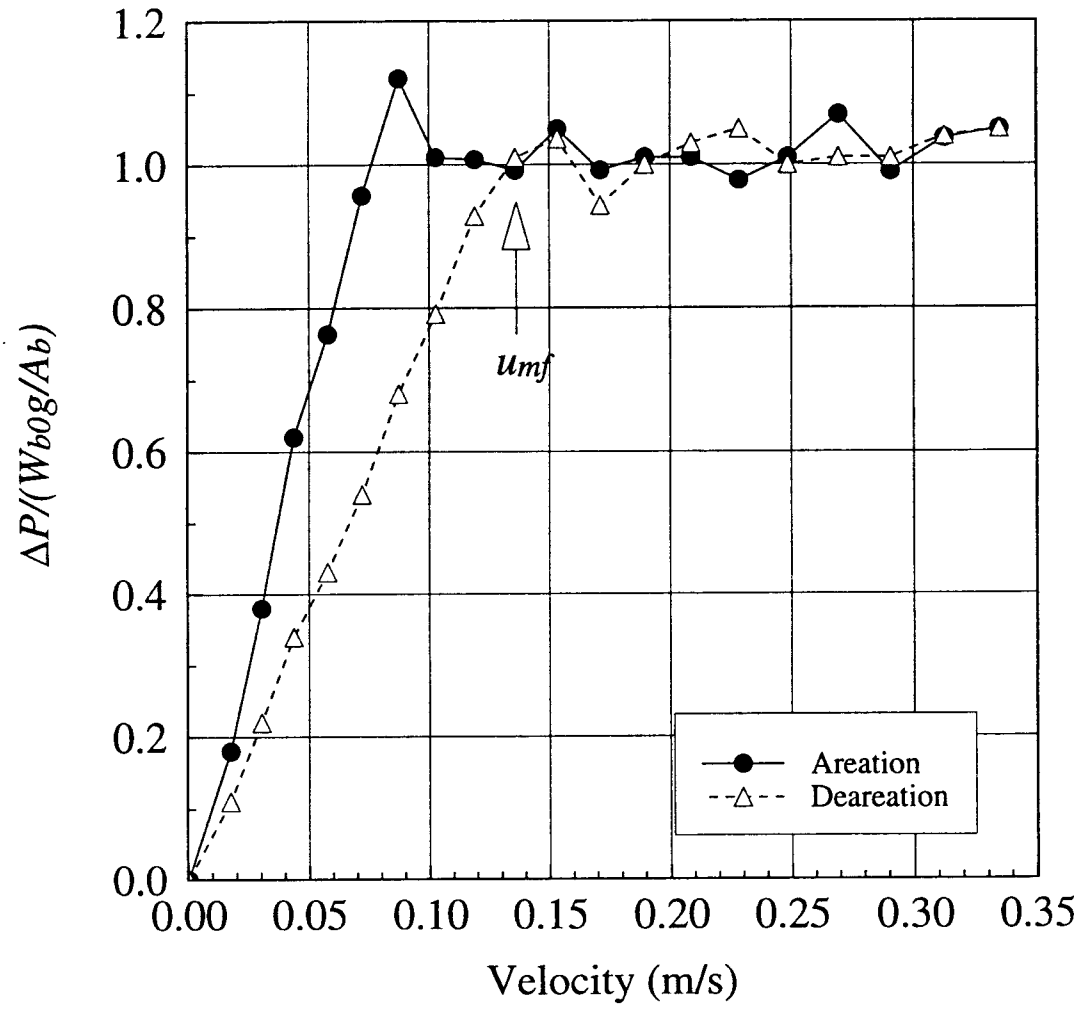

Figure 4.1 Normalized pressure drop across a fluidized bed containing 113.6 g of Si_3N_4 large particles.

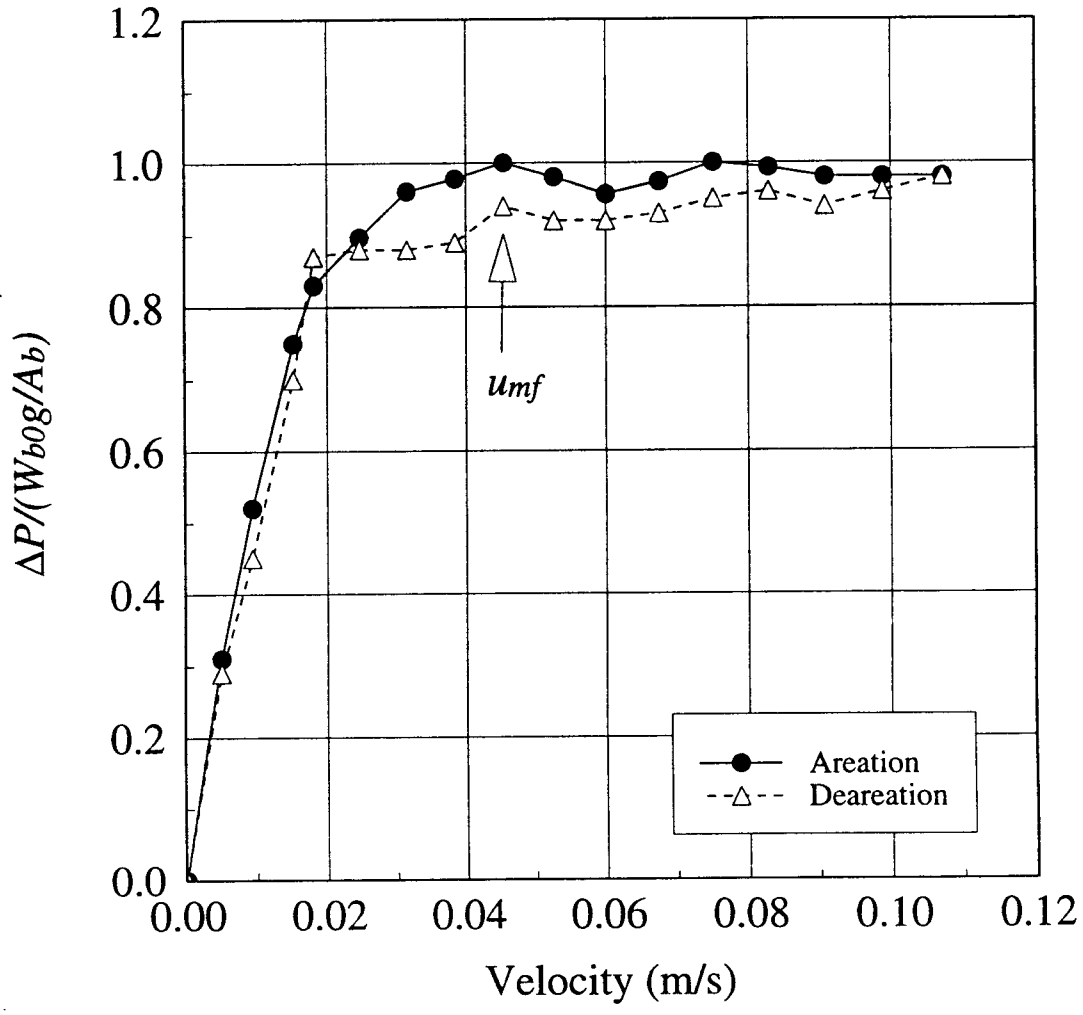

Figure 4.2 Normalized pressure drop across a fluidized bed containing 105.4 g of Si_3N_4 fine powders.

case. In the following kinetic study, the superficial gas velocity, u_0 was set at 1.5 times u_{mf} for smooth fluidization.

4.2 Observed Results

Because the furnace was removed during the kinetic study at the room temperature, the fluidizing phenomena were easily observed through the glass wall of the fluidized bed. The product was also taken out of the fluidized bed for examination after the reaction was terminated. These direct inspections provided better understanding of fluidization of the gas phase reaction of $SiCl_4$ and NH_3. The observed results are described below.

4.2.1 Reaction in a fluidized bed with large particles

The large Si_3N_4 particles, classified in Geldart B, were first tested as inert particles based on the findings that they are easy-to-fluidize without forming agglomerates and without entrainment. When two reactants were introduced into the fluidized bed at 300 K, with the gas velocity, u_0, set at 0.20 m/s (=1.5 × u_{mf}), smoke-like white powder formed in the trap flask, not in the bed. The smoke-like powder seemed to be the product blown out of the fluidized bed and caught by the trap flask. This phenomenon suggested that the residence time of the reactants in the bed was not long enough for the product to be generated within the fluidized bed. Even with an increased bed height and a reduced gas velocity, smoke still formed in the trap flask.

Thus, it was concluded that fluidizing the large Si_3N_4 inert particles was not suitable for the collection of product powder in this study.

4.2.2 Reaction in a fluidized bed with fine powder

Because the fine powder has a lower minimum fluidization velocity, it is expected that the reactants have a longer residence time in the bed. Hence in preliminary experiments, the fine powder was tested with the gas velocity u_0 set at 0.0675 m/s. The observed results are described below.

The Si_3N_4 fine powder appeared to be sticky at the beginning of fluidization. A small portion of fine particles attached to the column wall after fluidization for approximately 20 minutes. However, the attached particles in the splash zone began to fall down after carrying out the reaction for 40 minutes. This indicates that the inter-particle forces changed due to the reaction product coating inert particles, leading to less sticky particles. Particles hardly adhered on the column wall and no white smoke rose within the column or formed in the trap flask during the reaction, indicating that most of the product was collected within the dense zone and the reaction in the freeboard zone was minor.

Compared to the large particles, fluidizing the Si_3N_4 fine powder made it easier to collect the product powder. Therefore, all the reaction experiments were carried out by using the Si_3N_4 fine powder.

4.2.3 Product distribution

After each experiment, the whole bed of particles were poured out for visual inspection. The mixture of inert and product powders behaved like loose sand. There was no change observed in the light tan color of particles although most of the product was collected by the Si_3N_4 fine powder. Only a few white clusters were found in the product mixture. It seemed that part of product coagulated to form these small clusters rather than to attach to the inert particles. This occurred especially when the inert particles were not well mixed due to channeling. However, the chemical analysis of product samples showed that 70-95 % of $SiCl_4$ vapor was converted to the product powder in the fluidized bed reactor, assuming completely mixed inert and product powders in this reactor.

The solid products were not only collected by the inert particles but also self-coagulated and deposited on surfaces within the fluidized bed. A lump of white deposit was usually found at the outlet of the $SiCl_4$ supply pipe and caused the plugging problem. Sometimes, twig-like white product was obtained when stable channels formed in the bed. All of these deposits seemed to have formed due to the locally high concentration of reactants. Therefore, the plugging on the $SiCl_4$ supply pipe had to be cleared off by tapping the tee on the stopper, and the stable channels to be broken by vibrating the fluidized bed just in time. The chlorine content in these coagulates was 2 to 4 times higher than that in the average product mixture. However, the total amount of chlorine in these white coagulates was less than 4% of the total chlorine collected in the bed.

4.3 Entrainment of Fine Powder

Entrainment and elutriation play important roles in the fluidization of very fine powder. In this kinetic study, it was observed that the inert particles and product fines were continuously elutriated from the dense region and blown out of the reactor, thus the mass of the fluidized bed decreased during the fluidization. The reaction was terminated before the loss of particles caused experimental errors. Therefore, the entrainment of particles was investigated to know when to stop experiments.

Figure 4.3 compares the cumulative mass (W_c) of entrained particles with and without the reaction. All these carryover particles were collected by a couple of trap flasks replaced every other 15 minutes. The cumulative mass W_c with no reaction increased at a constant rate. The constant attrition became more stabilized after fluidizing particles for 45 minutes. In order to predict the bed mass during the fluidization, the reaction was carried out in the constant attrition region. Thus, the reaction was initiated after fluidizing inert powder for 45 minutes. After the reaction was initiated, the entrainment with reaction became higher than that without reaction and increased linearly with reaction time. The attrition rate was evaluated by the slope of each straight line, which is 2.1×10^{-4} kg/min for the case with reaction and 1.0×10^{-4} kg/min for that with no reaction. After fluidizing for 145 minutes, the loss of bed mass for the case with no reaction was 7.7% of the initial bed mass (W_{b0}) and that with reaction was 14%.

The results of this experiment suggest that the bed mass at any time during the reaction can be determined from the particle attrition rate. Since all the entrained

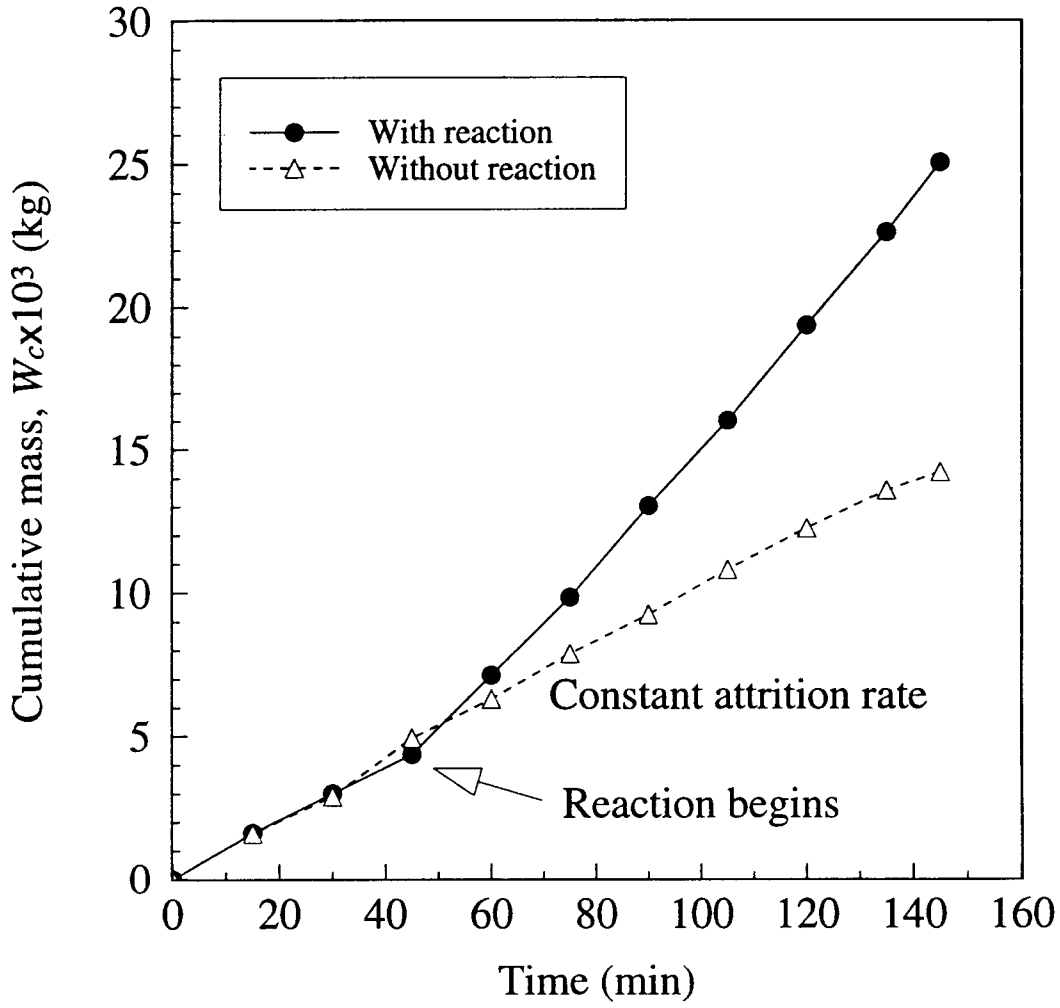

Figure 4.3 The accumulation of carryover fines versus time with W_{b0} = 182.5 g and u_0 = 0.0675 m/s.

particles were collected in the trap flasks at a constant attrition rate, the bed mass at any time during the reaction was expected to be the initial mass W_{b0} minus the mass of particles collected in the flask.

The effect of the reaction temperature on the entrainment of fines is shown in Figure 4.4. All the experiments were conducted using the same concentration of reactants ($SiCl_4$: 3.88×10^{-6} kmol/m^3, NH_3: 1.87×10^{-3} kmol/m^3). In each experiment, the reaction was started after the bed was fluidized for 45 minutes and then continued for 100 minutes. Figure 4.4 shows that the particle attrition rate in each run is essentially constant over the period of reaction. The higher the reaction temperature, the more the attrition. Figure 4.4 also shows that a higher attrition rate results from higher bed mass. The entrainment becomes more significant because increasing the bed mass shortens the freeboard zone. The total loss of bed mass after the fluidization with reaction is in range of 15-23% of the initial bed mass W_{b0}.

4.4 Analysis of Reaction Kinetics

4.4.1 Model description

The chlorine content in samples shows that the product mixture of $Si(NH)_2$ and NH_4Cl is collected by the Si_3N_4 fine powder in the fluidized bed. The solid products generated in the void space in the fluidized bed are considered to have deposited on the surface of the fluidized inert powder before being blown out. Since a little amount of powder having a high chlorine content was found on the filter paper, the collection of product generated in the bed may not be 100%. Also, previous research [4] help us

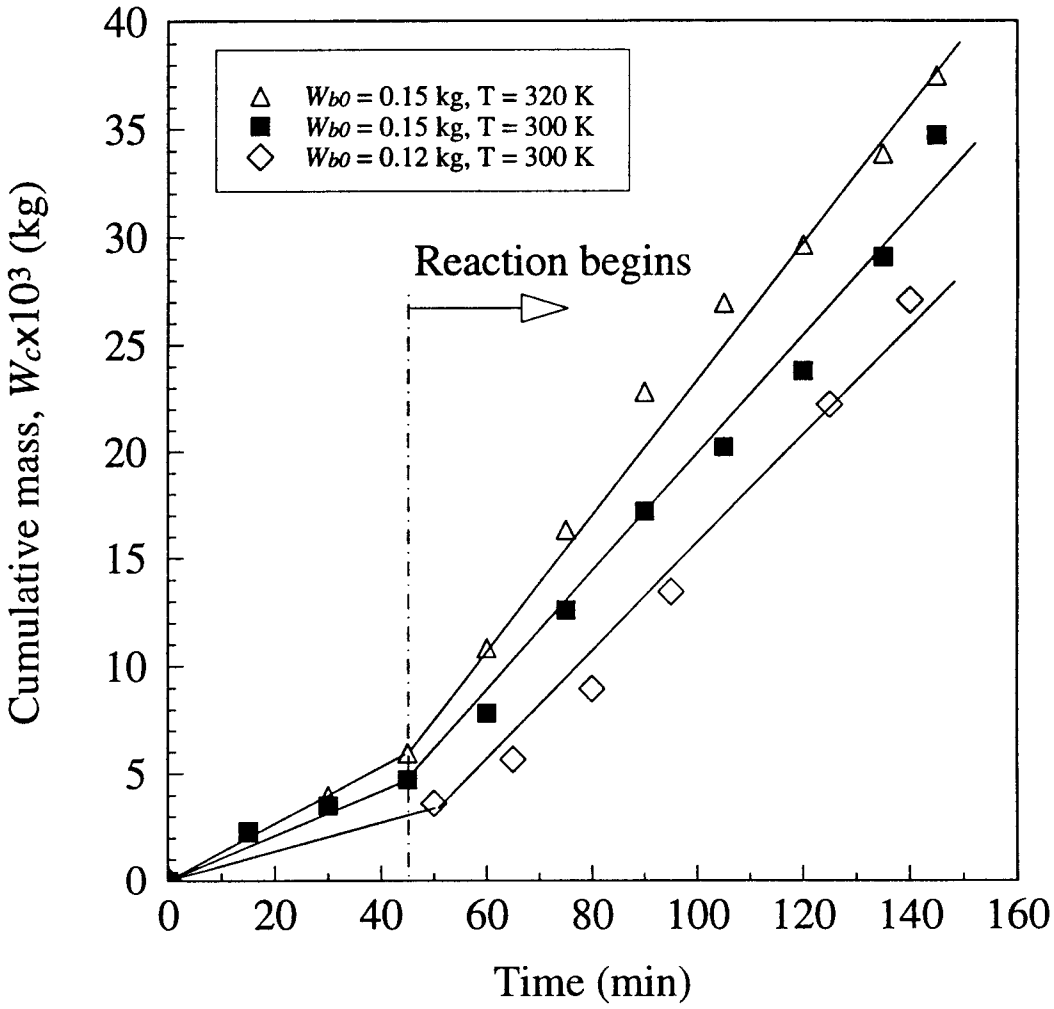

Figure 4.4 The temperature effect and bed weight dependence of cumulative Si_3N_4 fine powder.

to realize how fast the reaction is, and what may proceed inside the fluidized bed. Based on the experimental observation and the information obtained from the literature, a kinetic model to describe the reaction in the fluidized bed has been developed. The basic assumptions used in the present kinetic study are described below.

1. The reaction is carried out in the gas phase of the fluidized bed operated at the atmospheric pressure. The contribution of the heterogeneous surface reaction is negligible in comparison to the homogeneous gas phase reaction [3, 14].
2. Plug flow can represent the gas flow in the fluidized bed and the fluidized bed reactor can be considered as a tubular reactor.
3. Most of the solid products formed in the gas phase attach to the surface of fluidized particles. However, some of product particles that are not captured by the inert particles are entrained by the carrier gas. The efficiency f of collection is defined as

$$f = \frac{\text{moles of product remaining within the fluidized bed reactor}}{\text{moles of product generated in the void of the fluidized bed}} \qquad (4.1)$$

4. Fine particles are well mixed in the fluidized bed. The temperature and the concentration of product deposits are of uniform distribution throughout the fluidized bed.
5. The voidage of the bed, ε_A, is not affected by the system temperature [24]. It can be considered as a constant in the range of 280-353 K.

6. The stoichiometric ratio of $Si(NH)_2$ to NH_4Cl is always 1 to 4, no matter what mechanism the reaction at low temperatures follows.
7. Since NH_3 vapor is supplied in significant excess compared to $SiCl_4$ vapor, a pseudo-first order irreversible reaction with respect to $SiCl_4$ is assumed to be the reaction kinetics.
8. solid product attach instantaneously to the surface of inert particles after being formed in the gas phase reaction. The rate determined step in this case is the gas-phase reaction, not the product deposition.
9. The bed mass decreases with time due to the entrainment. However, since the decrease in bed mass is maintained small, at most 25% of the initial mass and 17% as average, the bed mass during the reaction is considered as a constant W_b, evaluated by taking an average of the bed mass before and after the reaction.

4.4.2 Model

Considering that only the gas phase reaction occurs between $SiCl_4$ and NH_4 in a fluidized bed, the conversion of $SiCl_4$ is defined as:

$$X_A = \frac{\text{moles of } SiCl_4 \text{ consumed}}{\text{moles of } SiCl_4 \text{ fed into the reactor}} = \frac{C_{A0} - C_A}{C_{A0}} \tag{4.2}$$

where C_{A0} and C_A are the inlet and outlet concentrations of $SiCl_4$, respectively. Based on assumptions 3, which considers the efficiency f of collection and on assumption 6, which assumes stoichiometric mixture of the products, the mass balance for $SiCl_4$ in the fluidized bed gives:

$$C_{A0}\, X_A'\, F = \frac{1}{4}\, R_d\, W_b \tag{4.3}$$

and

$$X_A' = f\, X_A \tag{4.4}$$

Where W_b is the average mass of bed over the reaction period, F is the total volumetric flow rate of gases entering the reactor, X'_A is the apparent conversion, and R_d is the molar rate of NH_4Cl deposition per unit mass of mixture particles. The factor of 1/4 is needed in equation (4.3) because one mole of $SiCl_4$ generates four moles of NH_4Cl. The rate of NH_4Cl deposition, R_d, may be expressed in terms of measurable quantities as:

$$R_d = \frac{1}{w}\,\frac{dN_{Cl}}{dt} \tag{4.5}$$

where w is the mass of sample solids taken from the fluidized bed each time for analysis, N_{Cl} is the molar content of chlorine in the sample and t is the reaction time. Combining Eqs.(4.3) and (4.5) gives X_A' as

$$X_A' = \frac{W_b}{4\, C_{A0} F}\left(\frac{1}{w}\,\frac{d\,N_{Cl}}{d\,t}\right) \tag{4.6}$$

According to assumptions 1 and 2, the performance equation of plug flow reactor is expressed by:

$$C_{A0}\, F\, dX_A = (-r_A)\, \varepsilon_A\, dV \tag{4.7}$$

where V is the bed volume, and ε_A is the bed voidage which can be determined from

an observed bed height H by the following equation:

$$\varepsilon_A = 1 - \frac{W_b}{\rho_s V} = 1 - \frac{W_b}{\rho_s A_b H} \tag{4.8}$$

where A_b is the cross sectional area of the bed.

Based on the assumption that the reaction follows a pseudo-first order kinetics with respect to $SiCl_4$, the rate of homogeneous reaction, $- r_A$, per unit void volume can be expressed as

$$-r_A = k_A C_A = k_A C_{A0} (1-X_A) \tag{4.9}$$

where k_A is the apparent rate constant. Substituting equation (4.9) and (4.4) into equation (4.7), and integrating the resultant equation yields

$$\ln (1 - \frac{X_A'}{f}) = - \frac{k_A \varepsilon_A V}{F} = - k_A \tau \qquad \text{with} \quad \tau = \frac{\varepsilon_A V}{F} \tag{4.10}$$

where τ is the resistance time of gaseous reactants. Because the value of f is not known, the model can be tested by plotting $1\text{-}X'_A$ against τ in a semi-log coordinate system and comparing with curves calculated with a number of estimated values of f. If the data fall on one of the curves for different values of f, then the suggested kinetics may describe the reaction system with a value of that curve.

4.4.3 Data analysis

In order to verify the model using experimental data, the experimental procedures and conditions were specifically designed. Firstly, a mixture of solid

products and inert particles were sampled and analyzed every 20 minutes to determine the amount of chlorine collected per unit mass of particles in the bed. The data were used to evaluate R_d by equation (4.5). Equation (4.3), derived from a mass balance of $SiCl_4$, was tested with respect to the constancy of f by varying C_{A0}. Thus, X'_A was determined from the slope of a linear plot of C_{A0} versus R_d. ε_A was estimated from the measurement of the bed height H, by changing the mass of bed, according to equation (4.8). The performance equation was also examined in terms of the influence of V on X_A', equation (4.10), and then to find f and k_A. Finally, the temperature effect on the rate of reaction was investigated.

Figure 4.5 shows the change in the content of chlorine in mixtures of solids at 300 K. Each experiment used the same initial amount of inert particles and an identical gas flow rate F. C_{A0} was varied in the range of 9.56×10^{-6}-4.99×10^{-5} kmol/m^3, while the concentration of NH_3 was kept at 1.87×10^{-3} kmol/m^3. The figure shows that in all the cases moles of chlorine per unit mass of solid (N_{Cl}/w) is proportional to the reaction time. The slope of each straight line represents the rate of deposition, R_d, as defined in equation (4.5).

Figure 4.6 shows the R_d values, determined from Figure 4.5, plotted against the inlet concentration C_{A0}. Since W_b and F are constant, a straight line passing through the origin indicates that equation (4.3) is valid and the collection efficiency is independent of C_{A0}. The slope of the line, which is determined to be 0.15, gives X_A' as 0.955, using $F = 1.05\times10^{-4}$ m^3/s and $W_b = 0.1585$ kg.

Measured results of V and ε_A are shown in Figure 4.7. In these experiments, the fluidization was carried out at 300 K with Si_3N_4 fine powder kept in the range of

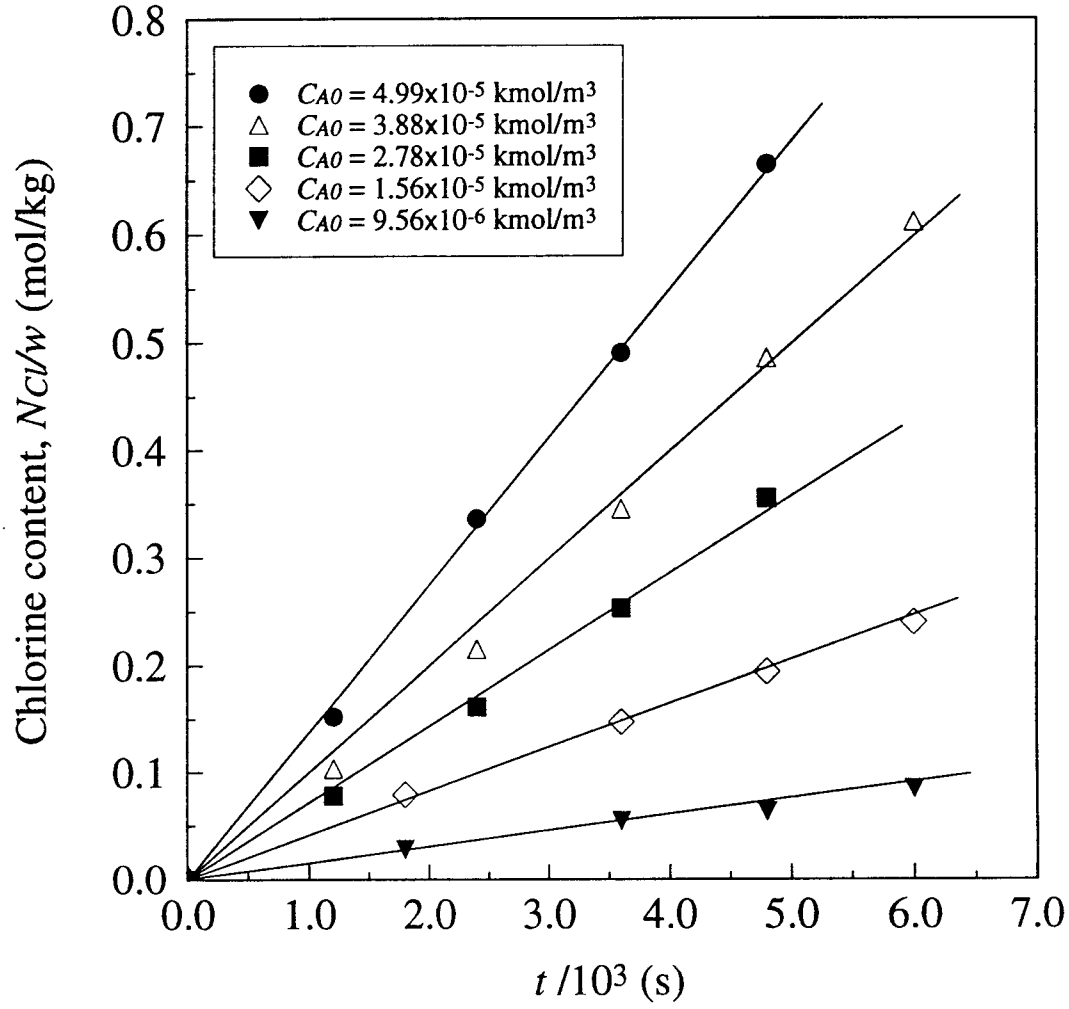

Figure 4.5 Time dependence of chlorine content of sample solids with W_b = 0.1585 kg.

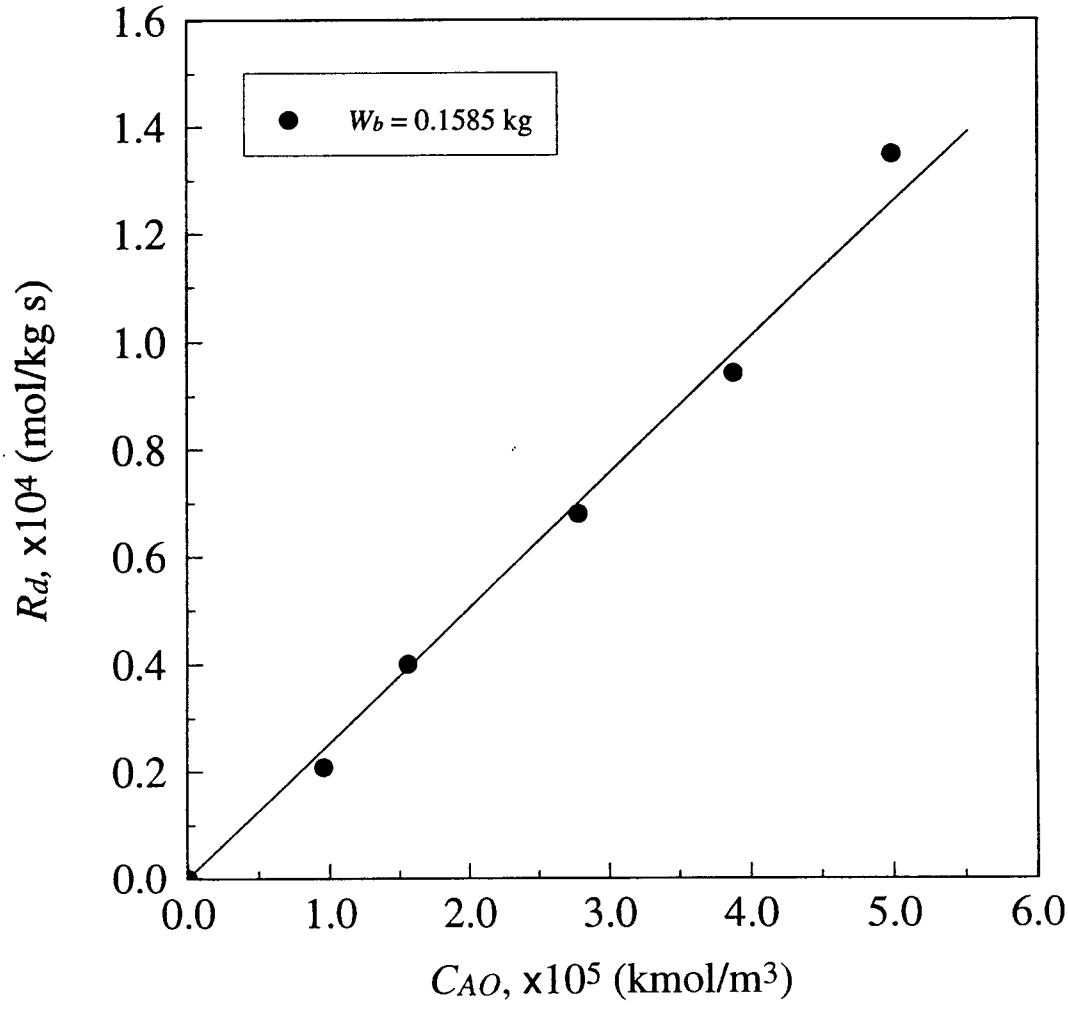

Figure 4.6 Deposition rate versus initial concentration of $SiCl_4$.

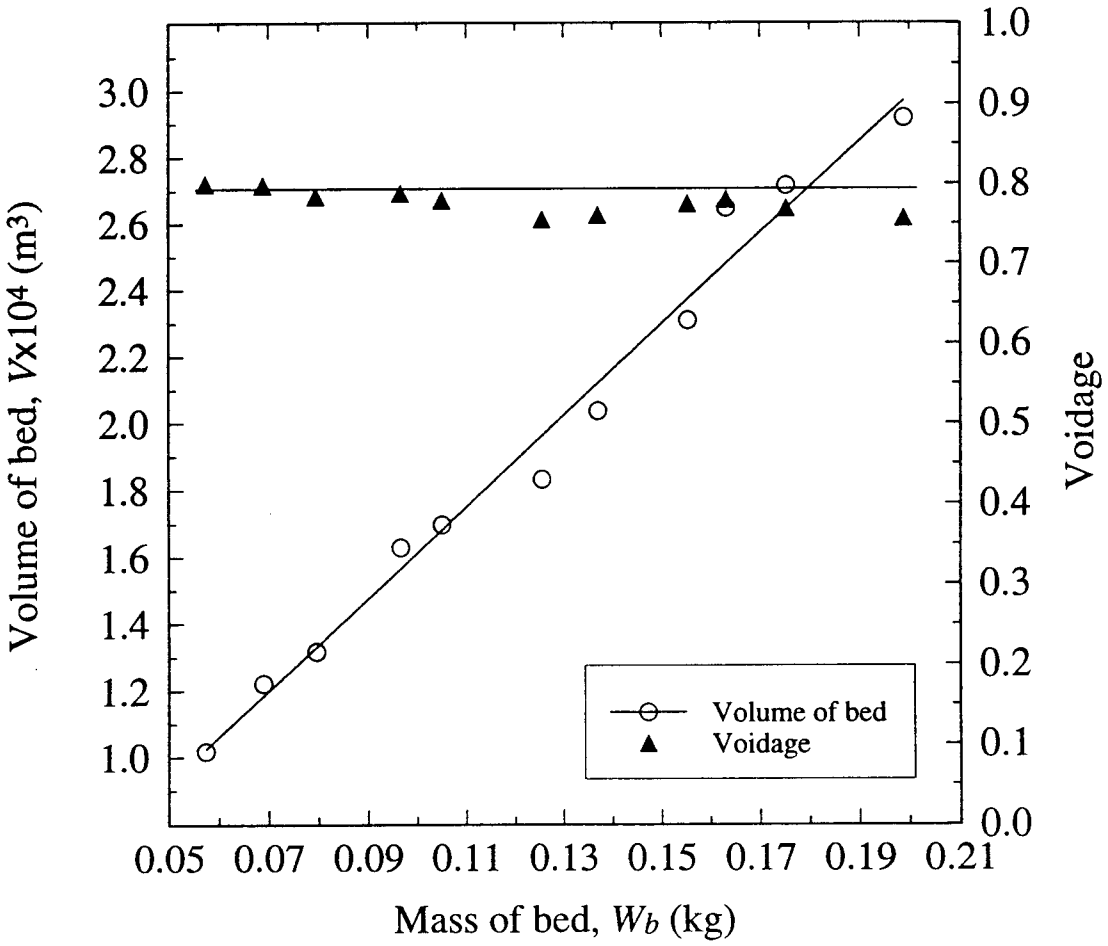

Figure 4.7 Measurements of volume of bed and voidage.

0.058-0.195 kg. The average bed height was measured by the height of the gas-solid mixture, defined as the distance from the gas distributor to the average level of splash zone (*i.e.* the fluctuating bed surface). The actual volume of the fluidized bed was calculated by subtracting the immersed volume of the $SiCl_4$ supply pipe from the measured bed volume (the bed height multiplied by the cross sectional area of the column). ε_A was then evaluated by equation (4.8). Since the ratio W_b/V was essentially constant, ε_A did not vary with W_b or V. The average ε_A was calculated to be 0.8 at u_0 = 0.0675 m/s.

Figure 4.8 illustrates the dependence of product deposition on the bed mass. In these experiments, W_b was changed from 0.1595 kg to 0.0676 kg. A minimum of 0.0676 kg was constrained by the failure of fluidization due to the formation of stable channels resulting from the short bed height less than 0.07 m. It is very interesting that R_d, the slope of straight line, decreases with W_b. Since the bed voidage ε_A is constant, as shown in Figure 4.7, V can be expressed as a function of W_b by rearranging equation (4.8). With the expression for V, equation (4.10) can then be written as

$$X_A' = f\left[1 - \exp\left(-\frac{k_A\ \varepsilon_A\ W_b}{\rho_s\ F\ (1-\varepsilon_A)}\right)\right] \tag{4.11}$$

Substituting equation (4.11) into equation (4.3) and solving the resultant equation for R_d yields a new expression of equation (4.3) in terms of W_b.

$$R_d = \frac{4\ C_{A0}\ F\ f}{W_b}\left[1 - \exp\left(-\frac{k_A\ \varepsilon_A\ W_b}{\rho_s\ F\ (1-\varepsilon_A)}\right)\right] \tag{4.12}$$

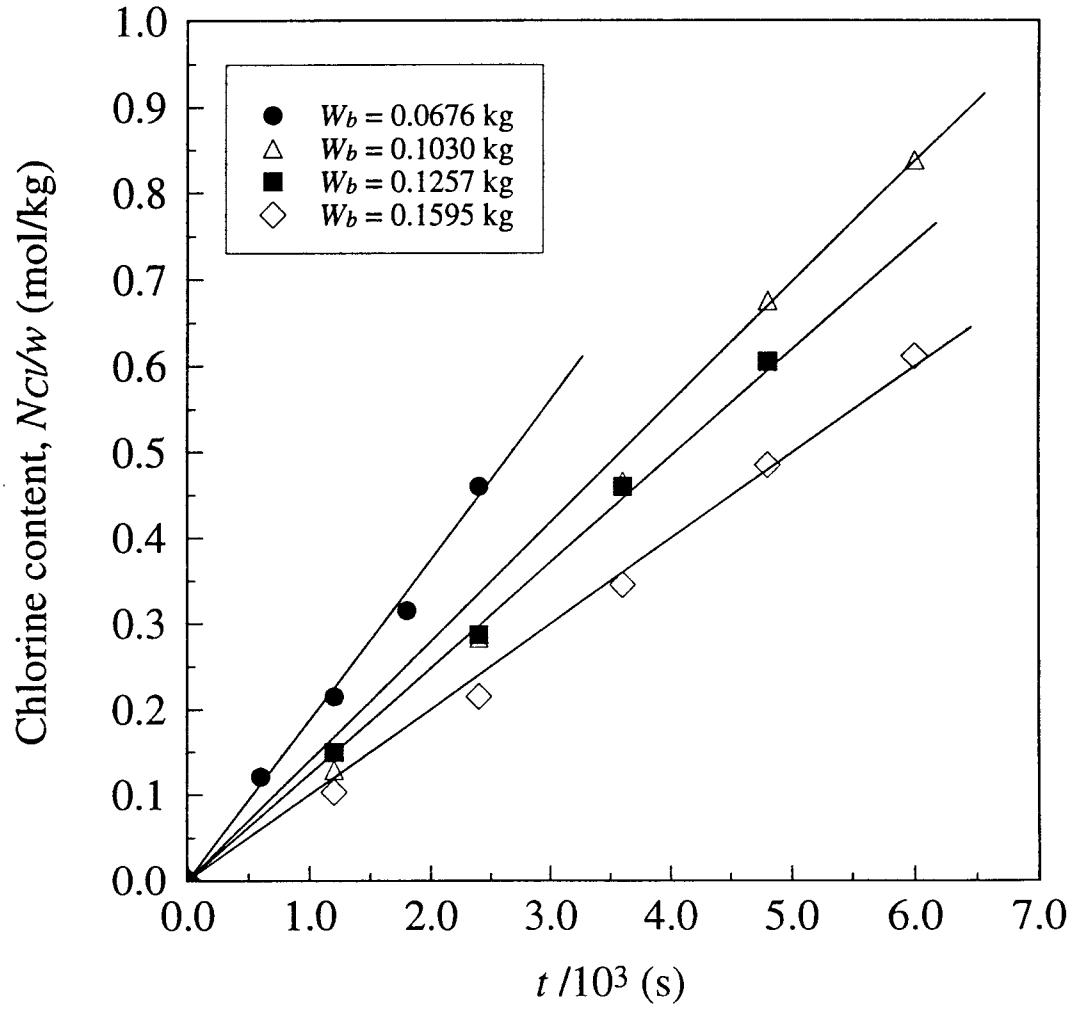

Figure 4.8 Bed weight dependence of product deposits.

According to the equation shown above, R_d decreases with the increase in W_b when the other variables, including f, in particular, are constant.

The proposed first order kinetics may be verified by plotting logarithm of $1\text{-}X'_A$ against τ as suggested by equation (4.10). The values of X'_A were determined by equation (4.6); τ for each corresponding X'_A was calculated by equation (4.10) using $\varepsilon_A = 0.8$. To find a set of k_A and f values that would best fit the $(1\text{-}X'_A)$ and τ data, a FORTRAN program to execute trial and error procedures was employed (see Appendix). Figure 4.9 displays the experimental data obtained at 300 K and the curve of $1\text{-}X'_A$ versus τ fitted with various f values. A value of $k_A = 1.55$ /s and a value of $f = 0.99$ give the best fit. Figure 4.10 shows a similar plot of $1\text{-}X'_A$ versus τ at 280 K. A value of $f = 0.98$ gives the best fit. Both values of f are very close to 1.0, which indicates that the efficiency of product collection is very high and is not affected by the reaction temperature. All the product powder formed in this fluidized bed is collected by the inert particles. Based on these tests, the value of f was assumed to be 1.00 in the following kinetic study.

The experiments to find the temperature dependence of the reaction were carried out in the range of temperature of 280-353 K. Figure 4.11 shows the plot of data obtained at 280, 300, and 320 K. Data obtained at 353 K were not included, because X'_A was found to be nearly 1.00. The rate of reaction at this temperature was so fast that $SiCl_4$ was totally converted within a short region close to the bottom of the bed. The value of k_A evaluated in Figure 4.11 from the slope of each line with $f =$ 1.00 may be plotted against the reciprocal of the reaction temperature to determine the activation energy for the pseudo-first order reaction. The Arrhenius plot shown in

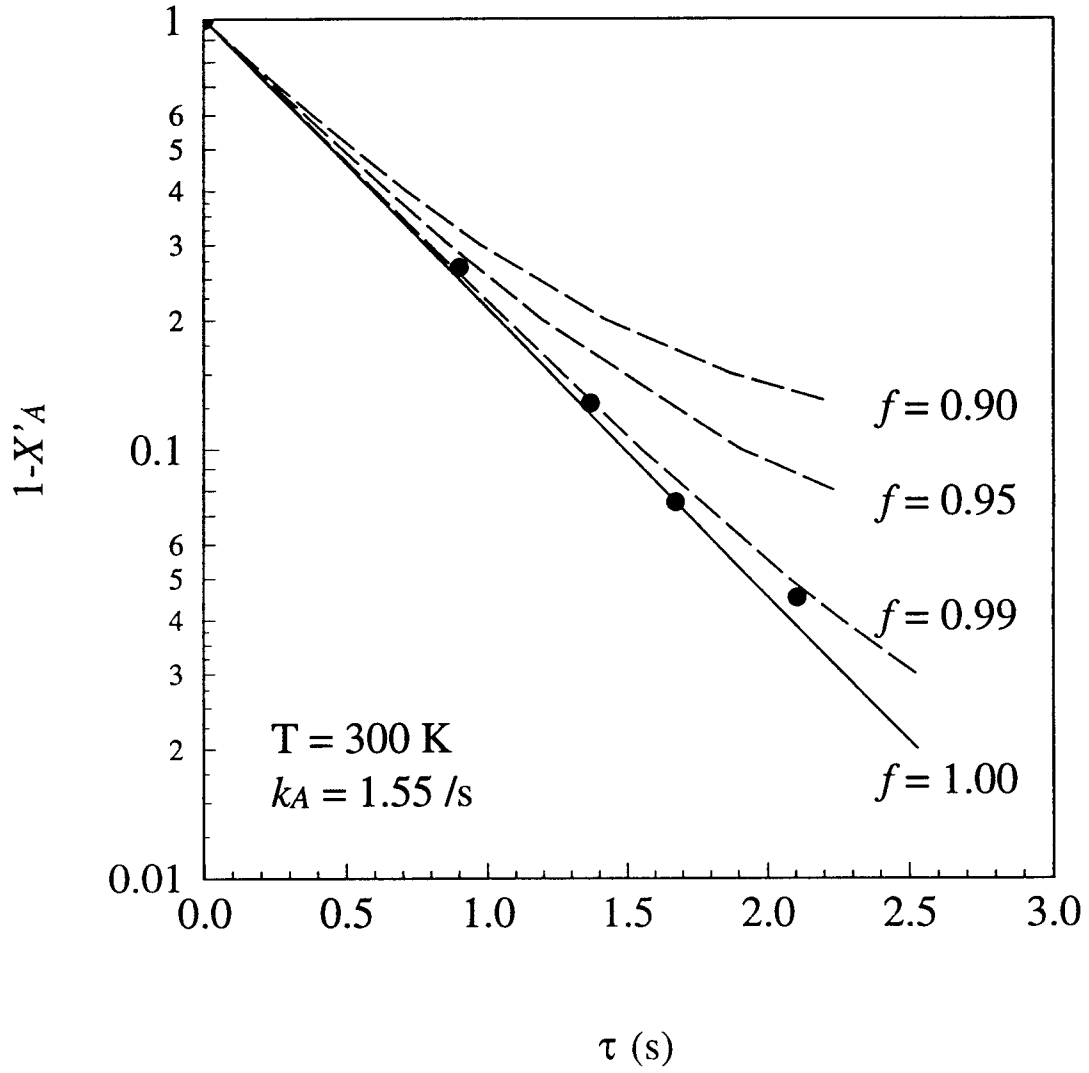

Figure 4.9 Test of plug flow model with pseudo-first order rate of reaction at 300 K, with the collection efficiency f varied.

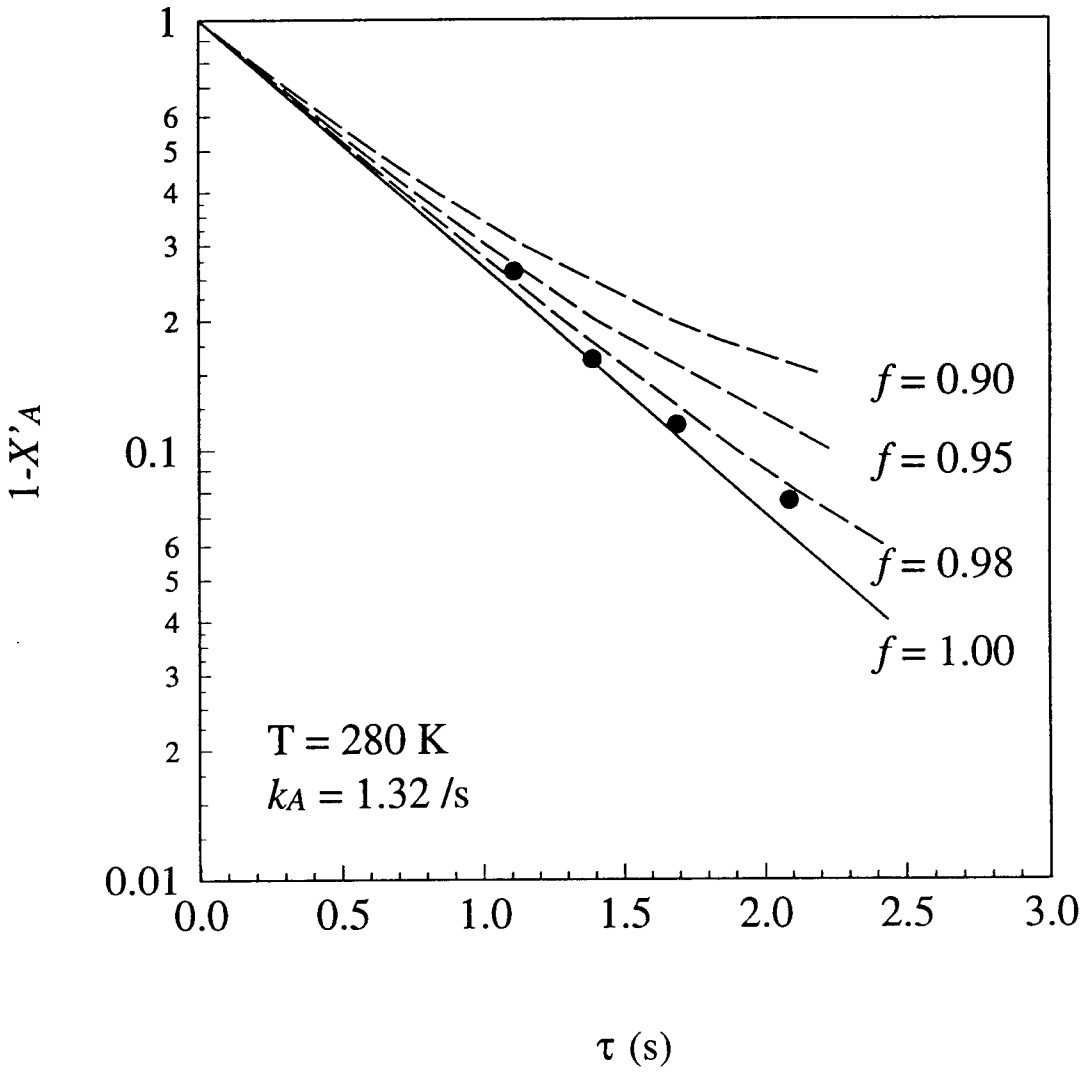

Figure 4.10 Test of plug flow model with pseudo-first order rate of reaction at 280 K, with the collection efficiency f varied.

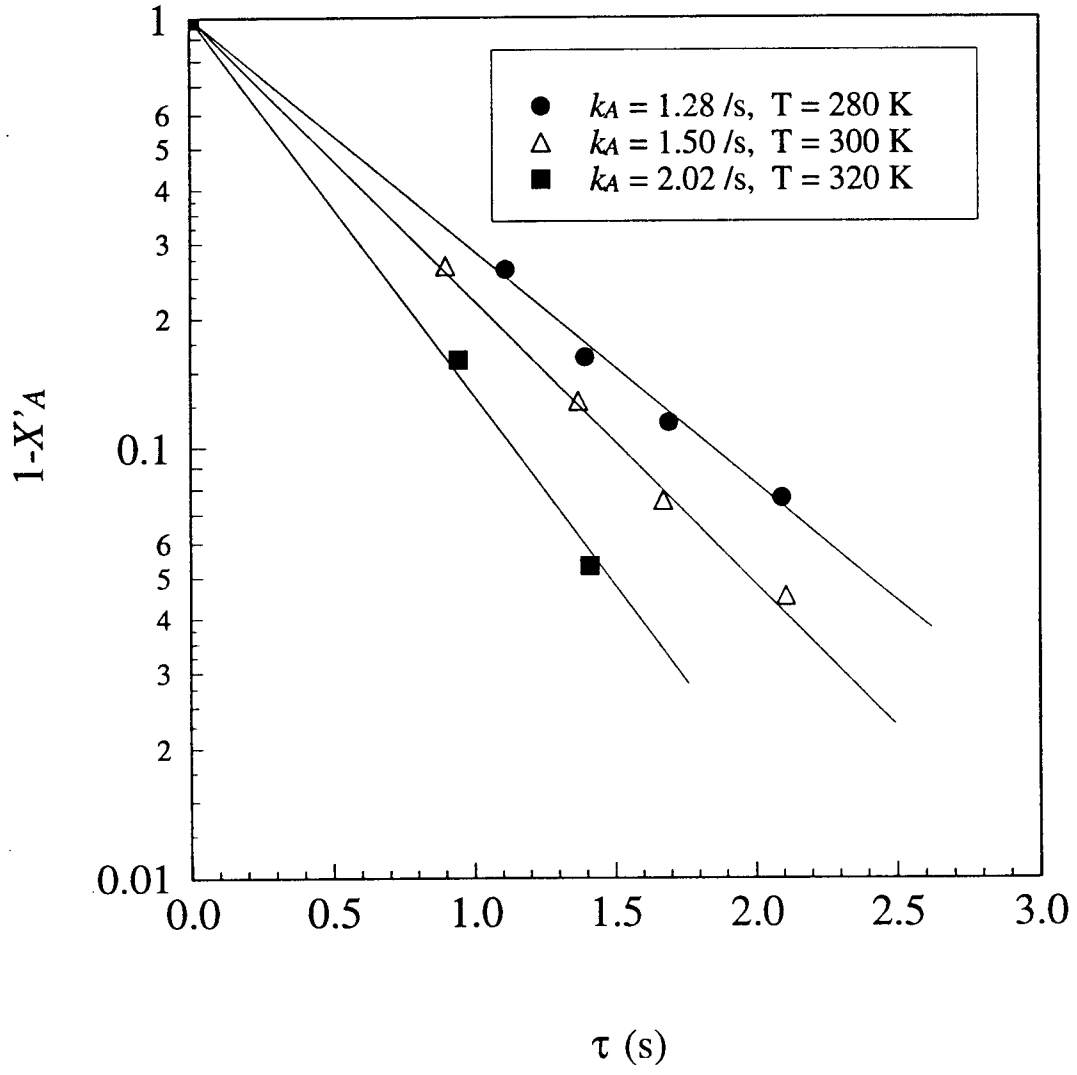

Figure 4.11 Test of plug model with pseudo-first order rate of reaction, with the collection efficiency $f = 1$.

Figure 4.12 gives the apparent activation energy of 8.40 kJ/mol, which is much smaller than the activation energy 62.7 kJ/mol reported in the literature [13]. However, the reaction mechanism at the room temperature may be different from that at high temperatures. This is considered to be the major reason for the large difference of the activation energies.

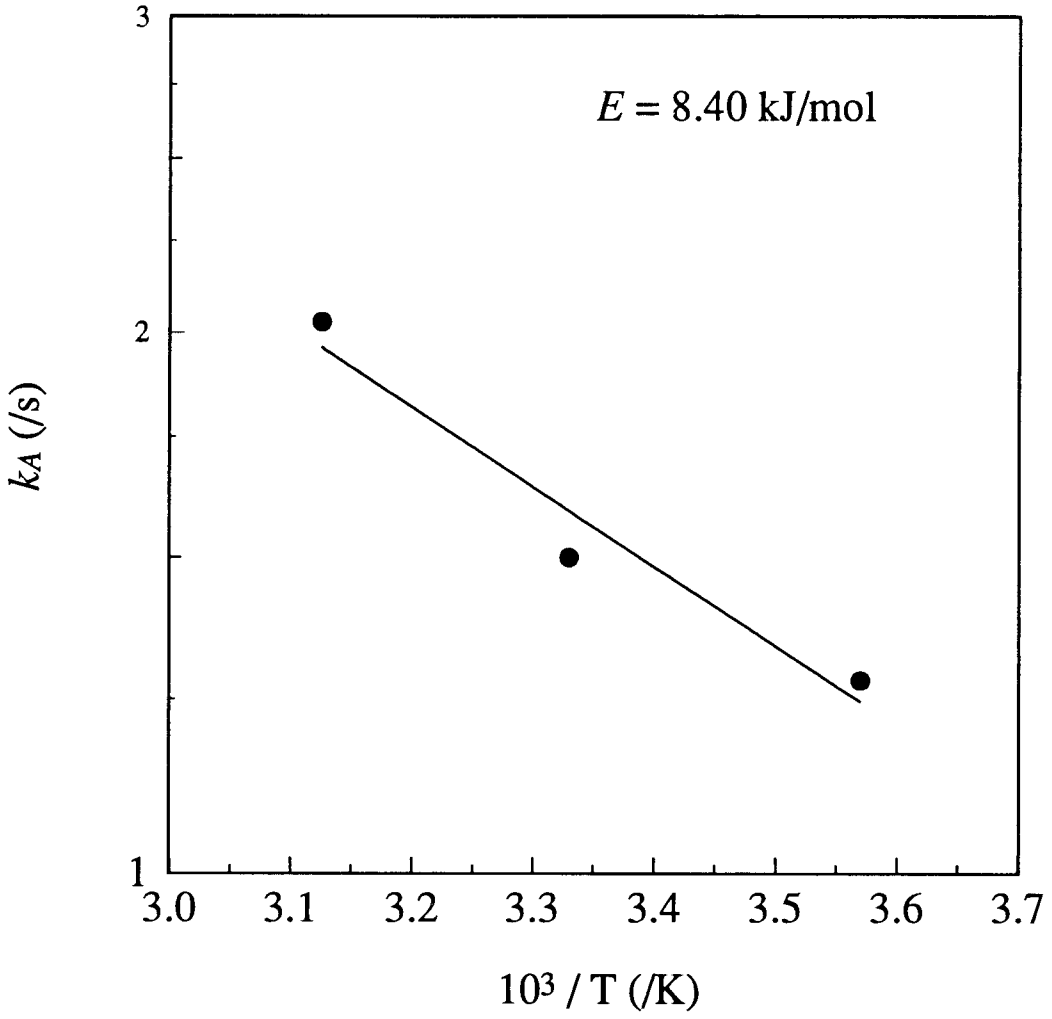

Figure 4.12 Arrhenius plot of the apparent rate constant k_A of the pseudo-first order reaction in a fluidized bed reactor.

CHAPTER 5

CONCLUSIONS AND RECOMMENDATIONS

5.1 Conclusions

The synthesis of $Si(NH)_2$ via the vapor phase reaction of $SiCl_4$ with NH_3 at temperatures close to the room temperature in a fluidized bed was investigated. Si_3N_4 particles having different average sizes were tested to collect product powder, a mixture of $Si(NH)_2$ and NH_4Cl. The entrainment of fine powder was measured under the conditions with and without the reaction at different temperatures. A model was proposed to describe the reaction forming the solid products. Experiments for studying the reaction kinetics were carried out to test the model and evaluate the rate constant. The results of this study may be summarized as below.

1. Fine Si_3N_4 powder (d_p = 0.5 μm) is suitable for collecting the product efficiently.
2. The attrition rate increases with the increase in the reaction temperature as well as with the increase in the molar flow rate of $SiCl_4$.
3. Product powder formed in the void of bed is almost completely (more than 98%) collected by the fine inert particles.
4. A plug flow reactor with a pseudo-first order rate equation with respect to $SiCl_4$ can represent the reaction in the fluidized bed reactor.
5. Apparent activation energy is 8.40 kJ/mol in the range of temperature of 280-320 K.

5.2 Recommendations for Future Work

In order to complete the development of Si_3N_4 synthesis via the gas-phase reaction of $SiCl_4$ with NH_3 at low temperatures around the room temperature in a fluidized bed, some recommendations for future work are given as below:

1. Modify the experimental apparatus to keep all the particles in the bed. A cyclone may be added to collect the entrained powder and feed back to the bed to maintain the amount of fluidized particles constant.
2. Investigate the effects of feeding locations and flow rates of $SiCl_4$ vapor to reduce the deposit at the outlet opening of the supply pipe.
3. Perform reaction (2.5) to synthesize Si_3N_4 by thermal decomposition of $Si(NH)_2$, step by step in a fluidized bed to test the feasibility of a continuous process.

BIBLIOGRAPHY

1. T. Yamada, "Preparation and Evaluation of Sinterable Silicon Nitride Powder by Imide Decomposition Method," *J. Am. Ceram. Soc. Bull.*, **72** [5] 99-106 (1993)

2. T. Yamada, T. Kawahito and T. Iwai, "Crystallization of Amorphous Si_3N_4 Prepared by the Thermal Decomposition of $Si(NH)_2$," *J. Mater. Sci. Lett.*, **2** 275-278 (1983)

3. T. C. Wang, "Impurity Chlorine in Si_3N_4 Produced Via Low Temperature Vapor Phase Reaction of $SiCl_4$ and NH_3," *M.S. Thesis*, Oregon State University, Corvallis, OR, (1991)

4. S. Morooka, A. Kobata and K. Kusakabe, "Rate Analysis of Composite Ceramic Particles Production by CVD Reactions in a Fluidized Bed," *Advances in Fluidized Systems AIChE Symposium Series*, **281** [87] 32-37 (1991)

5. M. Billy, "Preparation and Analysis of Silicon Nitride," (in Fri), *Ann. Chim. (Paris)*, **4** [13] 795-851 (1959)

6. G. M. Crosbie, "Silicon Nitride Powder Synthesis," *Proceeding of the 24th Automotive Technology Development Contractors' Coordination Meeting*, Society of Automotive Engineers, Warrendale, PA, 255-265 (1987)

7. K. Niihara and T Hirai, "Chemical Vapour-Deposited Silicon Nitride-*Part 2 Density and formation mechanism*," *J. Mater. Sci.* **11** 604-611 (1976)

8. K. Kasai, Y. Kubota, and T. Tsukidate, "Synthesis of α-Si_3N_4 Powders," *Yogoyo-Kyokai-Shi*, **88** [6] 358-359 (1980)

9. K. S. Mazdiyasni and C. M. Cooke, "Synthesis, Characterization, and Consolidation of Si_3N_4 Obtained from Ammonolysis of $SiCl_4$," *J. Am. Ceram. Soc.*, **56** [12] 628-633 (1973)

10. G. M. Crosbie, R. L. Predmesky, J. M. Nicholson and E. D. Stiles, "Prepilot Scale Synthesis of Silicon Nitride under Pressure," *J. Am. Ceram. Soc. Bull.*, **68** [5] 1010-1014 (1989)

11. Ford Motor Company, "Method of Making High-Purity Silicon Nitride Precursor," **U.S. Pat. No. 4,732,746** March 22 (1988)

12. M. Mitomo, H. Tanaka and J. Tanaka, "The Synthesis of α-Si_3N_4," *Yogyo-Kyoki-Shi*, **82** [2] 144-145 (1974)

13. M. J. Grieco, F. L. Worthing and B. Schwartz, "Silicon Nitride Thin Films from $SiCl_4$ Plus NH_3: Preparation and Properties," *J. Electrochem. Soc.: Solid State Science*, **115** [5] 525-531 (1968)

14. V. I. Belyi *et al.*,"Silicon Nitride in Electronics," *Mater. Sci. Monogr.*, **34** 41-45 (1989)

15. D. Geldart, "Types of Fluidization," *Powder Technol.*, **7** 285-292 (1973)

16. D. Geldart, N. Harnby and A. C. Wong, "Fluidization of Cohesive Powders," *Powder Technol.*, **37** 25-37 (1984)

17. J. Chaouki, C. Chauarie and D. Klvana, "Effect of Interparticle Forces on the Hydrodynamic Behavious of Fluidized Aerogels," *Powder Technol.*, **43** 117-125 (1985)

18. A. W. Pacek and A.W. Nienow, "Fluidization of Fine and very Dense Hardmetal Powders," *Powder Technol.*, **60** 145-158 (1990)

19. S. Morooka, K. Kusakabe, A. Kobata and Y, Kato, "Fluidization State of Ultrafine Powders," *J. Chem. Eng. Jpn.*, **21** [1] 41-46 (1988)

20. Y. D. Liu and S. Kimura, "Fluidization and Entrainment of Difficult-to-fluidize Fine Powder Mixed with Easy-to-fluidize Large Particles," *Powder Technol.*, **75** 189-196 (1993)

21. S. Morooka, T. Okubo and K. Kusakbe, "Recent work on fluidized bed processing of fine particles as advanced materials," *Powder Technol.*, **63** 105-112 (1990)

22. L. Marosi, "Vapor Phase Synthesis of Silicon Nitride from Silicon Tetrachloride and Ammonia," **Ger. Offen. DE 3,717,284** May 22 (1987)

23 B. H. Ayres, *Quantitative Chemical Analysis*, Harper & Row Press, New Yark, NY (1968)

24. D. Kunii and O. Levenspiel, *Fluidization Engineering*, Butterworth-Heinemann Press, Stoneham, MA (1993)

APPENDIX

LIST OF FORTRAN PROGRAM

Variable Listing

Program Symbol	Definition
AvCK	Algebra average of k_A values
CK	k_A values which are calculated by equation (4.9)
ER	Absolute error with respect to AvCK
f	f factor in equation (4.9)
I	Index of the experimental data sets
N, Nn	Number of experimental data sets
Tau	τ
XA	X_A

Program Listing

```
      Program kvalue
C
C.....  The purpose of this program is to find a set of (kA, f) which can best
C       fit the experimental data (Tau, XA). The method we used is a trial and
C       error procedure with absolute error criteria.  f is varied from 1.00 to
C       0.9 to seek a best kA value which has smallest absolute error.....
        Double Precision CK,F,XA,Tau,AvCK,ER,Nn
        Dimension CK(4),Tau(20),XA(20)
        Open (UNIT=2,FILE='HSU.DAT',STATUS='UNKNOWN')
C
C.....  Data input portion.....
        Write (*,*) ' Number of data points: '
```

```
      Read (*,*) N
      Do 10 I = 1, N
      Write (*,5) I
      Read (*,*) Tau(I)
      Write (*,6) I
      Read (*,*) XA(I)
   10 Write (2,7) I, Tau(I), I, XA(I)
      Write (2,8)
C
C.....kA value evaluation.....
      F = 1.0
      Nn = N
   40 AvCk = 0.0
      DO 20 I= 1, N
C
C.....The model equation solving for kA.....
            CK(I)= -DLOG (1-XA(I)/F) / Tau(I)
            Write (2,99) I, CK(I)
   20       AvCk = AvCk + CK(I)/ Nn
      ER = 0.0
      DO 50 I=1, N
C
C.....Absolute error evaluation.....
   50       ER = ER + ABS(((AvCk-CK(I))/AvCk*100000)/1000)
C
C.....Result output portion.....
      WRITE(2,999) F,AvCk,ER
            F=F-0.002
      IF(F.GT.0.8) GO TO 40
C
C.....Input data formate.....
```

```
    5   Format (' Tau(',I2,')=')
    6   Format (' XA (',I2,')=')
    7   Format (10X,' Tau(',I2,')=',F5.3,'  XA(',I2,')=',F5.3)
    8   Format (5X,60('='))
C
C.....  Output data formate.....
   99   Format (5X,'kA(',I2,')=',F8.3)
  999   Format (5X,'F= ',F6.4,8X,'Av kA=',E10.5,2X,'Error = ',F9.4,'%'/5X
     +        ,60('-'))
        STOP
        END
```

Output Data Listing

```
        Tau( 1)=1.110  XA( 1)= .740
        Tau( 2)=1.390  XA( 2)= .838
        Tau( 3)=1.690  XA( 3)= .886
        Tau( 4)=2.090  XA( 4)= .924
 ============================================================
 kA( 1)=   1.214
 kA( 2)=   1.309
 kA( 3)=   1.285
 kA( 4)=   1.233
 F= 1.0000        Av kA=.12603E+01  Error =   11.7284%
 ------------------------------------------------------------
 kA( 1)=   1.219
 kA( 2)=   1.317
 kA( 3)=   1.294
 kA( 4)=   1.245
 F=  .9980        Av kA=.12687E+01  Error =   11.6370%
```

---

kA(1)= 1.224

kA(2)= 1.325

kA(3)= 1.304

kA(4)= 1.257

F= .9960 Av kA=.12773E+01 Error = 11.5372%

---

kA(1)= 1.229

kA(2)= 1.332

kA(3)= 1.313

kA(4)= 1.269

F= .9940 Av kA=.12861E+01 Error = 11.4284%

---

kA(1)= 1.234

kA(2)= 1.340

kA(3)= 1.323

kA(4)= 1.282

F= .9920 Av kA=.12951E+01 Error = 11.3098%

---

kA(1)= 1.240

kA(2)= 1.348

kA(3)= 1.333

kA(4)= 1.296

F= .9900 Av kA=.13042E+01 Error = 11.1804%

---

kA(1)= 1.245

kA(2)= 1.356

kA(3)= 1.344

kA(4)= 1.309

F= .9880 Av kA=.13136E+01 Error = 11.0394%

---

kA(1)= 1.251

kA(2)= 1.364

kA(3)= 1.354

kA(4)= 1.324

F= .9860 Av kA=.13232E+01 Error = 10.9561%

---

kA(1)= 1.256

kA(2)= 1.373

kA(3)= 1.365

kA(4)= 1.338

F= .9840 Av kA=.13331E+01 Error = 11.5212%

---

kA(1)= 1.262

kA(2)= 1.381

kA(3)= 1.376

kA(4)= 1.354

F= .9820 Av kA=.13431E+01 Error = 12.1034%

---

kA(1)= 1.267

kA(2)= 1.390

kA(3)= 1.387

kA(4)= 1.369

F= .9800 Av kA=.13535E+01 Error = 12.7034%

---

kA(1)= 1.273

kA(2)= 1.398

kA(3)= 1.399

kA(4)= 1.386

F= .9780 Av kA=.13641E+01 Error = 13.3224%